THESIS

Forming the Hybrid Concept Design Grid

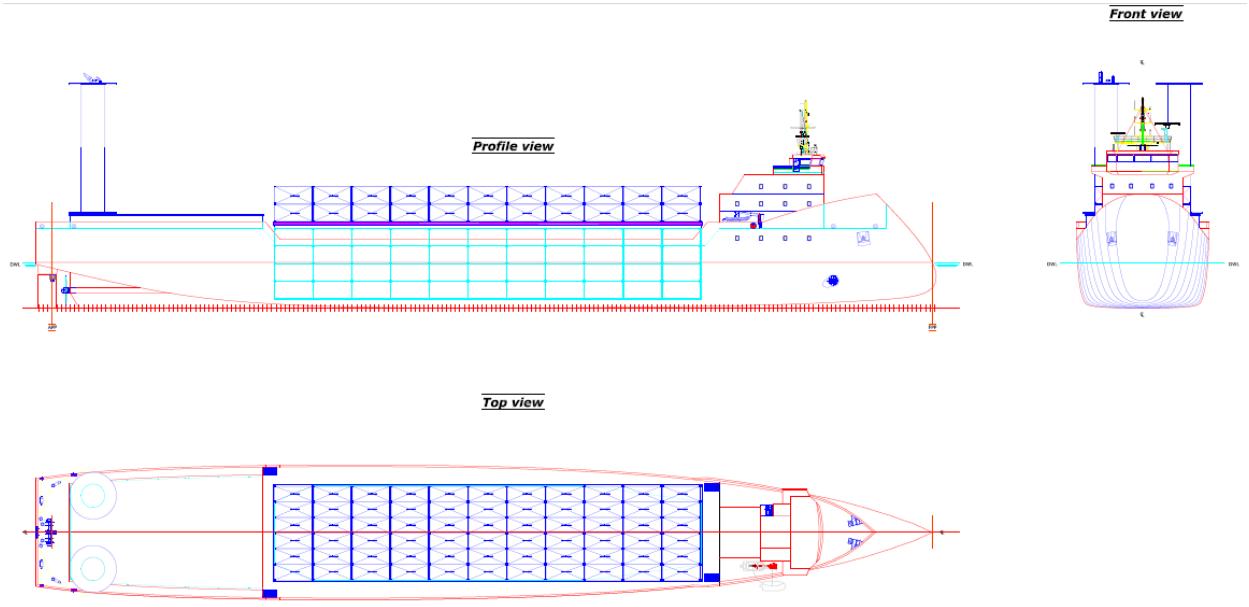

NHL HOGESCHOOL

C-JOB NAVAL ARCHITECTS / ENGINEERS

Declaration

I hereby declare that this thesis is my own work and effort and that it has not been submitted anywhere for any award. Where other sources of information have been used, They have been acknowledged.

Signature:.....

Date:.....

A hybrid sailing concept comparison (preliminary)

September 2013 – January 2014

C-Job & Partners BV
Madame Currieweg 29
8501 XC Joure
The Netherlands

Company advisor: Ir. J. Grijpstra
+31(0)23 56 20 768
j.grijpstra@c-job.eu

NHL Hogeschool
Maritime Engineering
Rengerslaan 10
8917 DD Leeuwarden
The Netherlands

Study advisor: Ing. E. Heijting
+31(0)58 25 11 176
e.j.heijting@nhl.nl

Graduate: Jethro R. de Vries
+31(6) 57 56 40 95
j.devries@c-job.eu
vrie0946@student.nhl.nl
jethrodevries@gmail.com

Kraneweg 91-D
9718 JL Groningen
The netherlands

Abstract

English

Is an application of the Magnus-effect in a hybrid sailing concept invest worthy in comparison with a conventional ship by equal operational profile?

The answer to this question has been obtained through the comparison of two suitable propulsion systems, the Flettner rotor and the Turbosail. Both systems use the Magnus-effect to gain Lift from axial rotation.Both systems have been implemented into a numerical concept design with an emphasis on specifying the hull form in relation to the cargo capacity, stability criteria and the cost estimation.

This numerical calculation and the final result have been compared with the conventional motorized general cargo ship, the AMELAND. This 7610 deadweight design sails at a ship velocity of 13 kts. These parameters have been used as criteria points for the Thesis and the calculation. Through the use of the performance data as provided by Charrier et al. the Flettner rotor and the Turbosail have been compared in the calculation on multiple lift coefficients, ranging from 2 to 8 for the Flettner rotor and from 2 to 6 for the Turbosail.

From these performance data follows the determination of the beam of the ship and the best suitable length solution by comparing multiple solutions of mast height, quantity of masts and the design lift coefficient. This results in a hull form that differs from the AMELAND by showing a lower Length-to-Beam ratio but with very low dimensionless hull coefficients. This reduces the resistance of the concept in relation to that of the AMELAND, which is necessary to gain the maximum lift coefficient for both concepts.

From the dimensions follows a construction cost calculation and an estimation of the operational costs in terms of fuel costs. After estimating the cargo profit the ROI of both the Flettner rotor and the Turbosail have been compared. From this comparison follows that both systems have a longer ROI than that of the AMELAND with a distinction between the systems in favour of the Flettner rotor.

Than the invest worthiness has been compared by looking at total profit after 15 years of service. Although both WASPs have an almost equal ROI, even in comparison to the conventional ship, the Flettner rotor has this profit at its maximal performance, while the Turbosail must sail with a minimal lift coefficient. The maximum profit with the Flettner rotor shows enough revenue to build a new ship.

Therefore the main thesis can be answered with yes, if a Flettner rotor would be installed on a 7610 tonnes dwt design.

Kind regards,

Jethro de Vries

Nederlands

Is het financieel aantrekkelijk om een toepassing van het Magnus-effect in een hybride concept te verwerken, in vergelijking met een conventioneel aangedreven schip bij gelijk operationeel profiel?

Het antwoord op deze vraag is behaald door een vergelijking te maken tussen twee bruikbare voortstuwingssystemen, de Flettner rotor en de Turbosail. Beide systemen maken gebruik van het Magnus-effect om Lift te genereren door axiale rotatie. Beide systemen zijn geïmplementeerd in een concept ontwerp met de focus op het specificeren van de rompvorm. Daarbij is gelet op de relatie tussen vracht capaciteit, stabiliteitscriteria en de kosten berekening.

Deze numerieke berekening en het uiteindelijke resultaat zijn vergeleken met die van het conventioneel gemotoriseerd aangedreven vracht schip, de AMELAND. Dit schip met een capaciteit van 7610 ton ladingsgewicht vaart bij een snelheid van 13 knopen. Deze gegevens zijn gebruikt als criteria punten voor de These en de berekening. Door het gebruik van de prestatiegegevens zoals gegeven door Charrier et al. zijn de Flettner rotor en de Turbosail met elkaar vergeleken op meerder lift coëfficiënten, variërend van 2 to 8 voor de Flettner rotor en van 2 tot 6 voor de Turbosail.

Van deze prestatie gegevens volgt de bepaling van de breedte van het schip en de meeste geschikte waterlijn lengte door verschillende oplossingen van de berekeningen met elkaar te vergelijken op mast hoogte, aantal masten en de ontwerp lift coëfficiënt. Dit resulteert in een rompvorm die aanzienlijk verschilt van die van de AMELAND. Dit blijkt uit een lagere lengtebreedte verhouding voor het concept maar wel lagere dimensieloze romp coëfficiënten. Dit verlaagd de weerstand in vergelijking met die van de AMELAND, dat noodzakelijk is voor het verkrijgen van de maximale lift coëfficiënt voor beide concept versies.

Vanuit de afmetingen volgt de berekening van de constructie costen en een schatting van de operationele costen in door de kosten van de brandstof. Na de schatting van de winst uit de lading is de ROI van het concept met de Flettner rotor en de Turbosail met elkaar vergeleken. Beide systemen hebben een iets langer ROI dan de AMELAND met het voordeel voor de Flettner rotor omdat deze zijn maximale lift coëfficiënt kan gebruiken.

Daarna is gekeken naar het investeringsperspectief door de totale opbrengst na 15 jaar te bekijken. Hoewel beide WASPs een vrijwel gelijke ROI hebben, zelfs in vergelijking met de AMELAND, blijkt de Flettner rotor doordat deze zijn maximale lift coëfficiënt kan benutten, de beste optie. Na 15 jaar blijkt dat er voldoende winst behaald is om een nieuw schip te bouwen.

Daarom word de Thesis dan ook beantwoord met ja, als de Flettner rotor wordt gebruikt bij een ladings gewicht van 7610 ton.

Met vriendelijke groet,

Jethro de Vries

Main Particulars

Particular	Concept	AMELAND	Unit
L_{oa}	140,00	122,10	[m]
L_{wl}	140,00	117,2	[m]
B	20,70	16,60	[m]
D	9,72	10,01	[m]
T_s	7,04	7,20	[m]
LSW	4762	4321	[t]
DWT	7620	7610	[t]
Δ	12382	11931	[t]

Acknowledgments

The subject of this thesis has been initiated by the SAIL project for which C-Job has been asked to design a concept. This has been linked to a study of two wind-assisted ship propulsion systems. This has been made possible by the C-Job office who has provided me with the necessary software and expertise to help me conduct the research regarding hybrid ship design.

In particular I want to thank Jelle Grijpstra from C-Job for his help and patience as my project advisor. The same counts for my project advisor from the NHL Hogeschool, Eric Heijting. Both have helped me by providing comments on my research and the final thesis rapport.

I want to thank all the C-Job colleagues at the C-Job office in Joure, for their assistance but also their kindness and humor. This has helped me to put the project into perspective.

I want to thank the members of the SAIL project for their help in divining my thesis question. I also want to thank them for their input in the score-matrix, which has helped me to select the most interesting wind-assisted ship propulsion systems.

Nomenclature

General

- Symbols are generally defined where they appear in the text for the first time.
- Units are generally put in brackets where they appear in the text.
- In-text references to chapters, paragraphs, tables or figures are italicized.
- Subscripts x, y, and z will denote directions in global coordinate system.
- The acceleration of gravity (g) is generally used as a constant, with value 9,81 [m/s^2].
- The seawater density (ρ_{sw}) is generally used as a constant, with value 1025 [kg/m^3].
- The air density (ρ_{air}) is generally used as a constant, with value 1,25 [kg/m^3]

Abbreviations

AR	Aspect Ratio
CFSS	Conventional Freight Sailing Ship
CLR	Centre of Lateral Resistance
COG	Centre Of Gravity
CONX	Constructional Costs
DWT	Deadweight
ETA	Estimated Time of Arrival
FW	Fresh Water
G.T.	Gross Tonnage
GA	General Arrangement
HAWT	Horizontal-Axis Wind Turbine
HC	Hatch Cover
HFO	Heavy Fuel Oil
HFSS	Hybrid Freight Sailing Ship
LC	Loading Condition
LNG	Liquefied Natural Gas
LO	Lube Oil
LSW	Light Ship Weight
MCR	Maximum Continuous Rating
MDO	Marine Diesel Oil
ME	Main Engine

MGO	Marine Gas Oil
OPEX	Operational Costs
ROI	Return On Investment
USD	American Dollars
VAWT	Vertical-Axis Wind Turbine
WASP	Wind-Assisted Ship Propulsion
WB	Water Ballast

Symbols

$\$_{LNG}$	Cost of the LNG
$\$_{MDO}$	Cost of the MDO [$]
$\$_{OPAX(lY)}$	OPAX costs of the previous year(s) [$]
$\$_{PROF(lY)}$	Profit of the previous year(s)
$\$_{PROF(y)}$	Profit [$]
(1+k1)	Pressure resistance coefficient
A_{BT}	Area of the bulb, forward of the intersection between the stem and the waterline [m^2]
$A_{DH(F)}$	Area of the deckhouse floors [m^2]
$A_{DH(O)}$	Area of the total deckhouse [m^2]
$A_{fcastle}$	Area of the forecastle deck [m^2]
A_{FrW}	Frontal wind area of the ship [m^2]
A_{hold}	Area of the cargo hold [m^2]
A_{hull}	Area of the hull up to the main deck [m^2]
A_{poop}	Area of the poop deck [m^2]
A_T	Area of the transom below the waterline [m^2]
A_{TD}	Area of the tween deck [m^2]
A_{TT}	Area of the tank top [m^2]
A_{WL}	Waterline area [m^2]
A_{WL2}	A waterline coefficient at a waterline that deviates from the T_S
A_{WT}	Area of the watertight frames [#]
B	Max breadth of the ship [m]
$B_{fcastle}$	Maximum Breadth of the forecastle deck [m]
B_{hold}	Cargo hold breadth [m]
B_m	Moulded Beam [m]

BM_t	Transverse metacentric radius [m]
B_n	Beaufort number
B_{TT}	Breadth of the tank top [m]
C_a	Aspiration coefficient
C_A	Correlation allowance coefficient
C_a	Power insertion coefficient
C_B	Block coefficient
C_{B2}	A block coefficient at a waterline that deviates from the T_S
C_{BD}	Block coefficient up to the main deck
C_{BTD}	Block coefficient up to the tween deck
C_{BTT}	Block coefficient up to the height of the tank top
C_D	Drag coefficient
C_F	Friction coefficient
C_H	Heel coefficient
C_L	Lift coefficient
C_{Lmax}	Maximum lift coefficient [-]
C_M	Midship area coefficient
C_{MC}	Mid-ship section coefficient in upright condition
C_P	Prismatic coefficient
C_{PD}	Prismatic coefficient up to the main deck
C_{stern}	Stern coefficient
C_T	Thrust coefficient
C_{WL}	Waterline coefficient
C_{WL2}	A waterline coefficient at a waterline that deviates from T_S
C_{WLD}	Waterline coefficient up to the main deck
C_{WLTD}	Waterline coefficient at the height of the tween deck
C_{WLTT}	Waterline coefficient at the height of the tank top
D	Depth [m]
f_{cIE}	Correction coefficient of i_E
F_D	Drag force [kN]
F_D	Drag force [kN]
F_F	Resulting force [kN]
F_H	Heel force [kN]
F_L	Lift force [kN]

F_L	Lift force [kN]
f_{LSW}	Correction coefficient of the Light Ship Weight
F_n	Froude number
F_{ni}	Froude number based on the immersion
F_{nT}	Froude number with the immersed transom
G	Centre of gravity
GM_t	Transverse metacentric Height [m]
GM_t	Transverse metacentric radius [m]
h_B	Height of the center of area of the bulbous bow above the keel line [m]
h_{DB}	Double bottom height [m]
h_{DB}	Height of the double bottom [m]
$h_{DH(L)}$	height of the deckhouse above the poop deck (main deck) [m]
$h_{fcastle}$	Height of the forecastle deck above the main deck [m]
H_{hold}	Cargo hold height [m]
H_m	Height of the WASP [m]
H_m	Height of the WASP [m]
h_{poop}	height of the poop deck above the main deck [m]
h_{trip}	Trip duration time [h]
i_E	halve angle of entrance of the water at the bow [°]
K	Specific volumetric weight for equipment and outfitting [t/m^2]
KB	Vertical center of buoyancy above the keel line [m]
KG	Vertical center of gravity above the keel line [m]
$KG_{container}$	Vertical center of gravity of the containers [m]
KG_{crew}	Vertical center of gravity of the crew [m]
$KG_{DH(F)}$	Vertical center of gravity of the deckhouse floors [m]
$KG_{DH(F)}$	Vertical center of gravity of the deckhouse floors [m]
$KG_{DH(O)}$	Vertical center of gravity of the complete deckhouse [m]
$KG_{E\&O}$	Vertical center of gravity of the equipment and outfitting [m]
$KG_{fcastle}$	Vertical center of gravity of the forecastle deck [m]
KG_{FO}	Vertical center of gravity of the fuel oil [m]
KG_{hatchc}	Vertical center of gravity of the hatch cover [m]
KG_{hold}	Vertical center of gravity of the cargo hold [m]
KG_{hull}	Vertical center of gravity of the hull [m]

KG_{LO}	Vertical center of gravity of the lube oil [m]
KG_{M}	Vertical center of gravity of the machinery [m]
KG_{MDO}	Vertical center of gravity of the marine diesel oil [m]
KG_{ME}	Vertical center of gravity of the main engine [m]
KG_{MGO}	Vertical center of gravity of the marine gas oil [m]
KG_{poop}	Vertical center of gravity of the poop deck [m]
KG_{SPAR}	Vertical center of gravity of the spare parts [m]
KG_{steel}	Vertical center of gravity of the steel [m]
KG_{TD}	Vertical center of gravity of the tween deck [m]
KG_{TT}	Vertical center of gravity of the tank top [m]
KG_{WASP}	Vertical center of gravity of the WASP [m]
$L_{a(APP)}$	Length of the ship aft of aft perpendicular [m]
lcb	Longitudinal center of buoyancy [% L_{wl} forward of mid-ship]
lcb	Longitudinal center of buoyancy [m] or [% L_{wl} forward of mid ship]
LCG	Longitudinal center of gravity forward of aft perpendicular [m]
$LCG_{container}$	Longitudinal center of gravity of the containers [m]
LCG_{crew}	Longitudinal center of gravity of the crew [m]
LCG_{DH}	Longitudinal center of gravity of the complete deckhouse [m]
$LCG_{E\&O}$	Longitudinal center of gravity of the equipment and outfitting [m]
$LCG_{fcastle}$	Longitudinal center of gravity of the forecastle deck [m]
LCG_{FO}	Longitudinal center of gravity of the fuel oil [m]
LCG_{hatchc}	Longitudinal center of gravity of the hatch cover [m]
LCG_{hull}	Longitudinal center of gravity of the hull [m]
LCG_{hull}	Longitudinal center of gravity of the hull [m]
LCG_{LO}	Longitudinal center of gravity of the lube oil [m]
LCG_{MDO}	Longitudinal center of gravity of the marine diesel oil [m]
LCG_{MGO}	Longitudinal center of gravity of the marine gas oil [m]
LCG_{poop}	Longitudinal center of gravity of the poop deck [m]
LCG_{SPAR}	Longitudinal center of gravity of the spare parts [m]
LCG_{steel}	Longitudinal center of gravity of the steel [m]
LCG_{TD}	Longitudinal center of gravity of the tween deck [m]
LCG_{TT}	Longitudinal center of gravity of the tank top [m]
L_{ch}	Chord length of the WASP [m]
L_{chE}	Length of the aft elliptical part of the Turbosail [m]

$L_{fcastle}$	Length of the forecastle deck [m]
L_{hold}	Cargo hold length [m]
L_{oa}	Length overall [m]
L_{poop}	Length of the poop deck [m]
L_{pp}	Length of the ship between the perpendiculars [m]
L_R	Resistance length [m]
L_{TD}	Length of the tween deck [m]
L_{TT}	Length of the tank top [m]
L_{wl}	Length on the waterline [m]
M_H	Heel moment [kNm]
N	Number of crew [#]
$n_{DH(F)}$	number of floors in the deckhouse [#]
n_{WT}	Number of watertight frames [#]
P_B	Bow immergence [m]
P_{MCR}	Power of the main engine at MCR [kW]
P_{SH}	Shaft power [kW]
q_{air}	Dynamic pressure of the air [kN/m^2]
q_{air}	Dynamic pressure of the air [kN/m^2]
q_{sw}	Dynamic pressure of the sea water [kN/m^2]
R	Bilge radius [m]
R_A	Additional resistance [kN]
R_{air}	Air resistance [kN]
R_{air}	Air resistance [kN]
R_B	Resistance from the bulbous bow [kN]
R_e	Reynolds number
R_F	Frictional resistance [kN]
R_F	Frictional resistance [kN]
r_h	Heel arm [m]
R_p	Pressure resistance [kN]
R_R	Residuary resistance [kN]
R_T	Total resistance [kN]
R_T	Total resistance [kN]
R_{TR}	Resistance from the submerged transom [kN]
R_W	Wave making resistance [kN]

R_W	Wave-making resistance [kN]
R_{water}	Water resistance [kN]
R_{water}	Water resistance [kN]
S	Reference area [m^2]
S_W	Wetted surface [m^2]
$S_{Wc\varphi}$	Wetted surface of the hull under a heel angle [m^2]
T	Draught [m]
t	wall thickness [m]
T2	A draught other than T_S [m]
T_f	Draught at the position of the forward perpendicular [m]
T_s	Scantling draught [m]
U	Apparent wind velocity [m/s]
V	Ship velocity [m/s]
V_f	Flow velocity [m/s]
W	True wind velocity [m/s]
$W_{container}$	Weight of the containers [t]
W_{crew}	Weight of the crew [t]
W_{DO}	Weight of the diesel oil [t]
$W_{E\&O}$	Weight of the equipment and outfitting [t]
W_{FO}	Weight of the fuel oil [t]
W_{LO}	Weight of the lube oil [t]
W_M	Weight of the machinery [t]
W_{SPAR}	Weight of the spare parts [t]
W_{steel}	Steel weight [t]
W_{WB}	Weight of the water ballast [t]
α	Tangential angle between C_L and C_D [°]
Δ	Displacement [t] or [m^3]
Δ	Displacement [tons]
η_D	Power efficiency from the main engine to the propeller
ν	Kinematic viscosity [m^2/s]
ρ_{air}	Density of the air [t/m^3]
ρ_g	Density of the gas [t/m^3]
ρ_{HFO}	Density of the heavy fuel oil [t/m^3]
ρ_{MDO}	Density of the marine diesel oil [t/m^3]

ρ_{sw}	Density of sea water [kN/m^2]
φ	Heel angle [°]
ψ_a	Apparent wind angle [°]
ψ_t	True wind angle [°]

Table of Contents

1 Introduction

1.1 Motivation

On Wednesday[I] October 24, 2012 the Interreg project IVB named SAIL has started. The goal of the project SAIL, hereafter referred to as SAIL, has been to stimulate and facilitate the transition process toward a sustainable shipping sector with focus on zero emission freight sailing. Why? Because the rate at which fossil fuel is being drained causes a threat to future global economy. Moreover the draining of the world's oil reserves will increase the oil prices drastically in the years to follow. Next to that, the burning of fossil fuel itself is undesirable because of the major environmental impact due to the release of NOx and SOx, that has been polluting the air. Especially the maritime shipping sector has been responsible for about[II] 20% of the global NOx and almost 92% of the global SOx emissions. Next to that about an annually amount of CO_2 of a 100 billion tons has been released. This has been caused mainly by the use of heavy fuel oil, a distillate or residue of petroleum distillation. It has been no wonder that the global society has agreed upon the importance of durable transportation. The International[III] Maritime Organisation, hereafter referred to as IMO, has reflected this opinion by demanding a drastic reduction in the amount of emissions for sea going vessels within the next 20 years, which will be included in the MARPOL ANNEX VI.

The issue could be solved by using cleaner alternative types of oil or by filtering the exhaust gases. But both options have a time limit because the oil supply will run out. Another solution could come in the form of gas, more specific Liquefied Natural Gas, hereafter referred to as LNG. The burning of LNG causes almost no NOx and SOx emissions at all. But just as the oil supply will run out, natural gas will run out in time as well. Therefore these solutions can only be seen as clean ways to postpone the search for green-energy solutions.

Another way to step into this problem is by Integrating a Wind-Assisted Ship Propulsion that allows a reduction of the emission within the sailing period of the ship. Wind sailing has been done for thousands of years without the use of electricity. Eventually sail ships became obsolete because they could not be kept at a competitive level in comparison with steam ships and eventually fossil fuelled ships. But nowadays most of these issues could be fixed because of various new available and optimized technologies.

One of the concepts that has been literally trying to integrate sails into a freight ship, has been the 130[IV] meter Ecoliner, at the moment of writing on the drawing boards at Dykstra Naval Architects. Analysis of the[V] hull shape shows a theoretical 18% cost reduction in comparison with a conventional motor ship. But this concept uses an ancient wind-propulsion mechanism in an improved form. A more radical way of wind propulsion has been the adoption of mechanical sails. "In 1926[VI], Anton Flettner replaced the sails on a

[I] Regarding this and the following cf. SAIL Website (n.d.)
[II] Regarding this and the following cf. Gendron and Trouvé (2013)
[III] Regarding this and the following cf. IMO Website (n.d.)
[IV] Regarding this and the following cf. Fairtransport Website (n.d.)
[V] Regarding this and the following cf. The Ecoliner concept (n.d.)
[VI] Regarding this ad the following cf. Back to the future: Flettner-Thom rotors for maritime propulsion? (n.d.)

schooner by twin rotatable cylinders to exploit the Magnus effect. With it, Flettner managed to cross the Atlantic in record time. But the rapid expansion in the use of diesel engines and the very low price of hydrocarbon fuel meant, however, that further exploitation or development did not take place. At least not until the end of the 20th Century. An example of the modern day integration of the so called Flettner rotors has been the E-ship 1, developed by ENERCON. This RoRo-ship[I], used for transporting ENERCON wind turbine components, uses four Flettner rotors. According to ENERCON, the rotors account for more than 15 percent of the savings compared to same-sized conventional freight vessels. If the numbers are to be believed, a supertanker equipped with the E-Ship 1 technology could possibly save up to 9,000 tons of fuel (approx. 27,000 tons CO^2). This would roughly mean a savings of 5 million dollars per year.

In 1980[II], Captain Cousteau, Professor Lucien Malavard and Dr. Bertrand Charrier tried to improve the mechanism as introduced by Flettner. They described the concept of Flettner as unsuccessful. As opposed to Flettner they used a fixed cylinder that looked like a smokestack and functioned like an airplane wing. They used a movable shutter and a system of fan-drawn aspiration to push the efficiency of the Magnus effect beyond that of the Flettner Rotor. And after a number of tests, the Turbosail showed a thrust coefficient of 3.5 to 4 times that of the best sails ever built (Marconi or square types, i.e. ships of the American Cup or the Japanese wind propulsion system). These tests resulted in the design of a complete exploration vessel that would include the Turbosail. Cousteau and his team designed an innovative hull of aluminum, both lightweight and strong. The catamaran-like stern gave it stability while the monohull forward would split the swells better. The ship has been named Alcyone.

Both WASPs use the same phenomena that is known as the Magnus-effect, but in a different way. So far the systems have been tested on exploration vessels and Ro-Ro ships. But what about large container ships crossing the North Sea or shipping Transatlantic? The global shipping industry could only be convinced to using mechanical sails as a new way of propulsion if the technique would be reliable enough. This is really a financial issue. And because the technique has been verily new and the optimal integration will take time, the costs needed to be assessed.

This has been the main goal of the paper before you. It will be answering the thesis question:

Is an application of the Magnus-effect in a hybrid sailing concept invest worthy in comparison with a conventional ship by equal operational profile?

1.2 Outline

Appendix A shows the Project Proposal. This proposal has been used to define the project. This proposal was drafted with the idea that the propulsions systems could be integrated onto the existing hull form of the Ecoliner. Soon after the initiation of the project it became clear that the Ecoliner would not be available within SAIL and this project. Also the performance of the propulsion systems showed difficult to be obtained. Therefore the focus of this study has moved from, presenting the concept in drawing form, to a study of a

[I] Regarding this and following cf. ENERCON Press Release (n.d.)
[II] Regarding this and the following cf. Cousteau Website (n.d.)

suitable hull form with the use of a wind-assisted ship propulsion. Therefore this paper will hold a lot of numerical data. Because of this shift of focus, the calculation of rudder and propeller, as well as any route specific calculations have not been included. However, these changes have not effected the thesis question or the sub questions in any way.

Because the thesis criteria holds a propulsion system that uses the Magnus-effect, the effect will be explained within this paper.

The thesis question will be answered by studying several sub problems. The first one is the choice of what the concept in this study will include.

Secondly, the best suitable application of the Magnus-effect has to be chosen. In terms of propulsion a selection of such wind assisted ship propulsion mechanisms has been made. This requires a comparison based on several criteria points. The study will continue with the technical part of the comparison of the two options where the different criteria aspects will be used to set limits to the calculations.

This will be integrated into a hull form that will be described numerically. This calculation will be initialized by using the hull of the conventional freight ship to verify the calculations.

As an outcome of the calculations, the most suitable propulsion system will be chosen. The resulting hull parameters will be describing the difference between the conventional freight ship hull and the hybrid freight ship. The parameters will be used to model a 3D-hull form to see whether the results are realistic and whether the design will meet the stability criteria. The hull form will be presented in the *Lines Plan*.

As a final step a comparison between the conventional freight ship and the hybrid freight ship based upon the Return On Investment will be used to determine the success of the concept. This will include the savings on fuel and cost.

1.3 Methods

The study has been conducted by using a numerical analysis of the concept design. This numerical analysis has been done by integrating multiple calculations in excel. Reference to this calculation as a whole will be done by using the term, *ICALC*. Some formulae have been obtained by analysing a 3D model of the concept in the software package Maxsurf.

1.4 Demarcation

The outcome of the comparison of the wind assisted ship propulsion systems and the hybrid freight sailing ship and the conventional freight sailing ship has been based upon the financial evaluation. This financial evaluation does not take into account variances of the propulsion type costs and has been fixed at one million US dollars per item per propulsion system.

The results do not represent any specific route, but the results have been based upon an overall route condition.

The heel resistance of the ship has been taken into account, but not the induced resistance. The resistance due to trim effects of the wind assisted ship propulsion has not been included in the calculation.

No actual construction of the ship has been calculated, because the aim of the study has been the hull form of the hybrid freight sailing ship.

2 Wind-Assisted Ship Propulsion

A WASP is a Wind-Assisted Ship Propulsion hereafter referred to as a WASP. The hybrid concept which is the main object of the thesis question must hold a WASP. This leads to the sub question:

What type of wind-assisted ship propulsion based on the Magnus-effect is the most suitable for a hybrid freight sailing concept?

This has been determined by comparing the WASPs on different criteria points, hence the question:

How do the different wind-driven propulsion systems relate to each other?

The sub question also holds the criteria that the WASP must use the Magnus-effect. So let's see what this Magnus-effect is.

2.1 Magnus-Effect

The Magnus-effect has been[I] named after the physicist who first described the phenomenon that a spinning body deviates from an original course.

This effect can be explained by using *figure 2.1*. The figure shows that a non-rotating cylinder as seen in the top of *figure 2.1*, has equal stream lines on both of the cylinder. Then by spinning the cylinder, as represented in the bottom figure of *figure 2.1*, the gas flow suddenly becomes different on either side of the cylinder. As a product of that change the cylinder experiences a force called Lift, hereafter referred to as L. This force moves the object from its original course. L is also the force that pushes an non-rotating aerofoil upwards. The difference between the L of an aerofoil and a body that has L due to spinning, is that the body that uses the Magnus-effect does not have lift if the body would not rotate.

[I] Regarding this and the following cf. Encyclopaedia Britannica (n.d.)

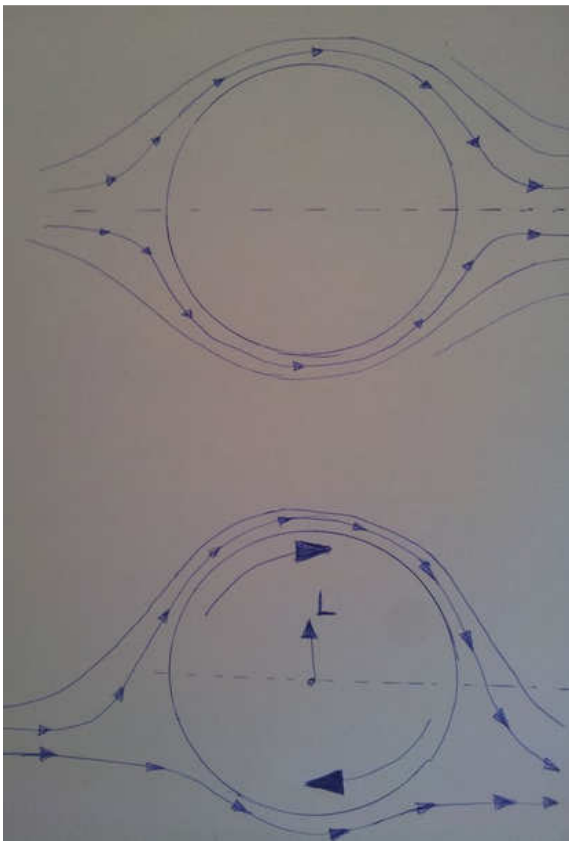

Figure 2.1: The Magnus effect on a rotating cylinder (Own Interpretation)

2.1.1 Lift

Both sides of the object have a specific air flow and a pressure acting on the object. This must be in accordance with the Bernoulli[I] equation, as seen in *equation 2.1*. This states that the initial *pressure* (p in kN/m^2) and the *dynamic pressure* (q in kN/m^2) that consists out of the *gas density* (ρ in t/m^3) and the *flow velocity* (v in m/s) are constant. That is in a frictionless environment. The longer flow lines in *figure 2.1* indicate a higher v on that side of the body, because of the longer translation in the same amount of time. Therefore a lower p must be the result on that side of the projectile.

$$p + \frac{\rho v^2}{2} = constant \tag{2.1}$$

But the deviation of the object from its original course must also comply with Newton's third law, action is reaction. This requires a constant change of pressure and velocity parameters in the surrounding gas of the object, else the object would appear to be in a static state and no L would move the object towards one side.

Somewhere between 1904 and 1906 the physicists Kutta in Germany and Zhukovsky in Russia tried to find the cause for this constant change of p and v. their answer has been

[I] Regarding this and the following cf. http://www3.kis.uni-freiburg.de/~peter/teach/hydro/hydro05.pdf (n.d.)

obtained by doing experiments where large scale circulation was added to a zero lift potential flow. This *circulation* (Γ m^2/s) has been defined by the integral around a closed curve in the fluid, and depends as seen in *equation 2.2* on the *fluid velocity* (v m/s) and the *length of the curve* (l in m)

$$\Gamma = \oint_c v \cdot dl \tag{2.2}$$

By comparing this to experiments where no circulation is used, the conclusion can be made that an irrotational solution of the air flow streaming around an object leads to a stagnation point on the trailing edge, where the velocity is infinite. *Figure 2.2* shows this solution in the top figure. Although this is a complex method, it can be shown that there is only one value for the circulation for which the flow speed is finite at the trailing edge and where the solution reflects the actual flow direction around the object witnessed in lift condition, as seen in the bottom figure of *figure 2.2.*

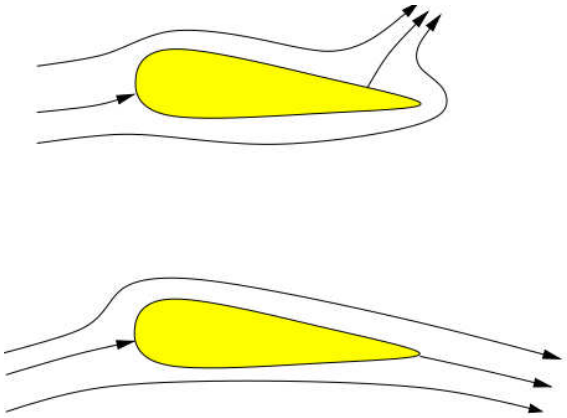

Top: Irrotational flow with vanishing circulation. Stagnation point upstream of the trailing edge, such that the velocity at the trailing edge is infinite.
Bottom: Solution with finite circulation and finite velocity at the trailing edge. It is natural to hope (Kutta-Joukowski-Hypothesis) that this particular flow will correspond to the steady flow that is actually observed.

Figure 2.2: Flow Around an Aerofoil (http://www3.kis.uni-freiburg.de/~peter/teach/hydro/hydro05.pdf)

Therefore the Kutta-Joukowski theorem has been based upon the relation between lift and circulation. The relation can be shown by using Bernoulli's equation for the pressure difference as given in *equation 2.3.*

$$p_b - p_t = \frac{1}{2}\rho(v_t + v_b)(v_t - v_b) \sim \rho V(v_t - v_b) \tag{2.3}$$

The *lift force* (F_L in kN) that moves the object away from the original course can be obtained as seen in *equation...* by integrating along the profile from the leading edge, x = 0, to the trailing edge, x = c.

$$L \sim \rho V \int_0^c (v_t - v_b)dx \tag{2.4}$$

But a reformulation of the circulation formula as seen in *equation 2.2* shows that L corresponds to the negative circulation around an aerofoil. This can be seen in *equation 2.5. Equations 2.4* and *2.5* thus results in the Kutta-Joukowski theorem as seen in *equation 2.6.* The previous calculations have thus shown that Lift can only be realized if there is a pressure difference on either sides of the body and that there is circulation.

$$\Gamma = \int_0^c v_b \cdot dx + \int_c^0 v_t \cdot dx = -\int_0^c (v_t - v_b) dx \tag{2.5}$$

$$L = -\rho U \Gamma \tag{2.6}$$

2.2 Available WASPs

There are two possible WASPs that use rotation in order to translate itself towards another position. The first WASP is a complete spinning body that therefore causes L in accordance with the theory as described in *paragraph 2.1.1 Lift*. The second option is a WASP that uses partial spin to enforce L.

2.2.1 Flettner rotor

The spinning rotor often referred to as a Flettner rotor or a Flettner-Thom rotor is a large mechanical sail. It is a rotating cylinder with or without so called Thom discs on the outer sides of the cylinder. The idea has been introduced in the early 20th century by Anton Flettner. Together[I] with Abert Betz, Jacob Ackeret, Ludwig Prandtl and Albert Einstein, Flettner constructed an experimental ship with the rotors installed. The ship as seen in *figure 2.3* was christened Buckau.

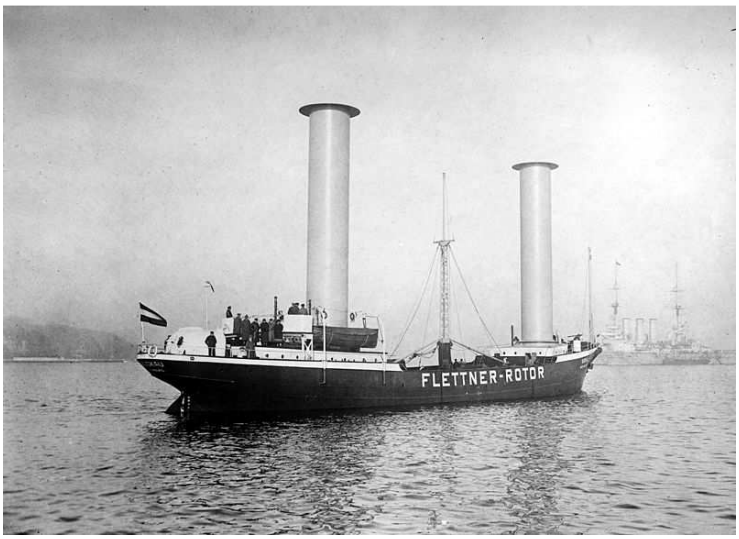

Figure 2.3: The rotor ship Backau, finished on October 1924 at the Germania Werft (http://www.thiiink.com/history-of-flettner-rotor/)

The L of the Flettner rotor depends mostly on the *axial velocity in reference to the flow velocity* (Ω), and by the *Aspect Ratio*, hereafter referred to as AR, between the *height of the* cylinder or *mast* (H_m in m) and the *chord length of the profile* (L_{ch} in m).

[I] Regarding this and the following cf. Thiiink (n.d.), website

2.2.2 Turbosail

The Turbosail, which started as an alternative design of the Flettner Rotor, was developed by Jacques-Yves Cousteau. Although the Turbosail does not rotate as a whole, L does depend on a rotating part of this WASP. Therefore this study does take this WASP as a propulsion system that uses the Magnus-effect.

Unlike the cylinder shape of the Flettner rotor, the Turbosail looks more like an aerofoil with its oval shape. *Figure 2.4* shows the different aspects of the Turbosail. As seen in this figure, the foil has a flap on the aft side of the profile. This flap can rotate to either side of the Turbosail, where it will close a vent opening on whatever side this flap is. Doing this ensures that the suction from the van in the hat only happens on one side of the profile to be exact, the side where L is desired. The suction of the boundary layer causes the stagnation point as seen in *figure 2.2* to disappear. The result is thus the same as with the axial rotation of the Flettner rotor, but the method is different.

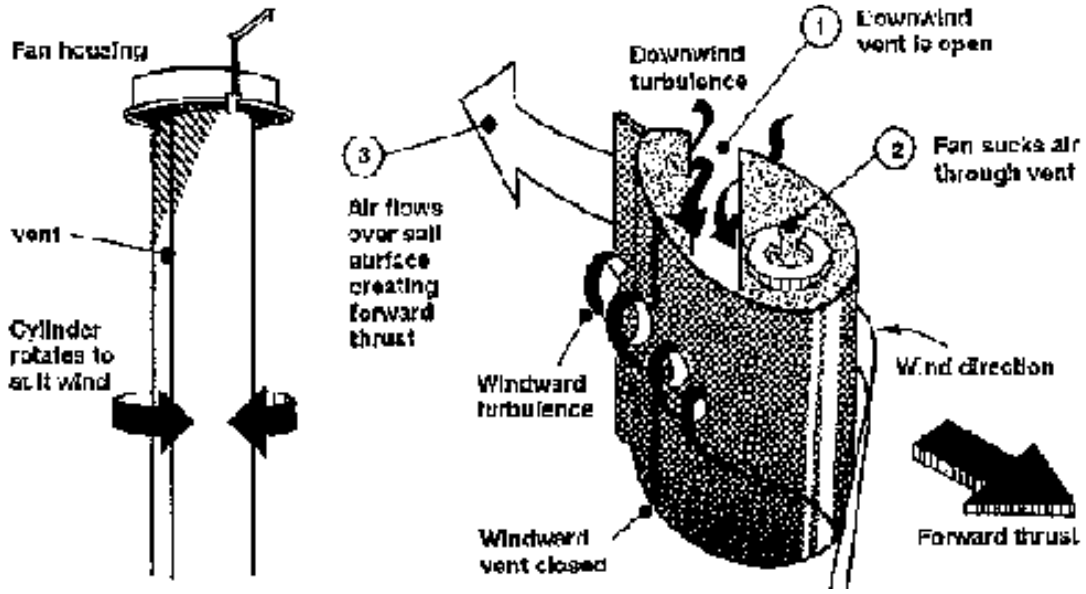

Figure 2.4: The working of the Turbosail (http://www.cd3wd.com/cd3wd_40/cd3wd/AGRIC/B19FIE/EN/B725_4.HTM)

2.3 WASP Integration Difficulties

There are a number of problems that every WASP has to overcome. And the success rate of each WASP depends on how those issues can be solved through the use of that WASP. The main issues regarding the use of WASPs over fossil fuelled engines has been the unpredictable ETA, crew size and skills, limited mechanical power on-board, costs and compliance with the modern standards of global trade. These problems could be overcome.

First of all, the ETA problem could be solved by using WASPs as an additional means of propulsion, instead of the WASP being the main propulsion type.

Secondly, the crew issue can be solved by using modern mechanical sails that require almost no monitoring. This is doable by using either the Flettner rotor and the Turbosail.

Thirdly, the mechanical power on-board can be provided by using an on-board generator that either uses clean fuel or is completely electric. This is a problem that will not be solved within this project.

Fourthly, The cost problem could be solved through the improvement of the Return[I] On Investment, hereafter referred to as ROI.

The main thesis states that the concept should be invest worthy. Although investors would want a ROI that is as short as possible, the concept would not be able to have an equal ROI in comparison to conventional ships, due to an added Beam and the cost of the WASPs.

Lastly, the HFSS could comply with the modern standards of global trade by integrating efficient loading and unloading mechanisms. Fortunately the Flettner rotor and Turbosail do not have a complicated rigging system that makes use of the entire deck. Therefore the loading and unloading issue is not applicable.

2.4 WASP Criteria Comparison

To assess which WASP is mostly desirable, criteria points must be given. This is what has been done in the SAIL project by means of the so-called Score-Matrix, as seen in *Appendix B.* This matrix uses several criteria points with a given weight factor in the range of 1-3, where the importance increases with the number. The WASPs have been given a score for each specific criteria point in the range of 1-5, where the higher number represents a higher strength of that WASP for that criteria. The results of this objective comparison as seen in *table 2.1* shows that there is a higher expectation of success for the Turbosail over the Flettner rotor.

This is interesting because since the late 80's the Flettner rotor has been integrated in multiple concepts, while the Turbosail received almost no attention. A WASP study in the 80's also discarded the Turbosail for being inefficient, by looking at the *maximum lift coefficient* (C_{Lmax}) as seen in *figure 2.5.* The Turbosail can be found as the 'Moulin A Vent' in *figure 2.5.*

[I] Regarding this and the following cf. Gernez (2010)

	Weight Factor	Turbosail	Flettner rotor
Cost	2,3	2,2	2,5
Performance (Lift Coefficient)	2,8	3,8	4,2
Performance (Lift/Drag Ratio)	2,5	4,0	3,0
Uptime/Downtime	1,7	3,2	2,7
Operability	2,6	4,7	5,0
Place taken on the Deck	2,6	4,0	4,0
Weight/Volume of System	1,7	2,6	2,8
Automation Opportunities	2,6	4,8	4,6
Robustness	2,7	4,2	3,3
Wind load	1,4	3,0	3,0
Impact on Stability	2,0	3,3	3,3
Technological Matureness	1,6	1,8	1,8
Total Average Score		**83,0**	**81,6**

Table 2.1: Score-Matrix Results (SAIL Project)

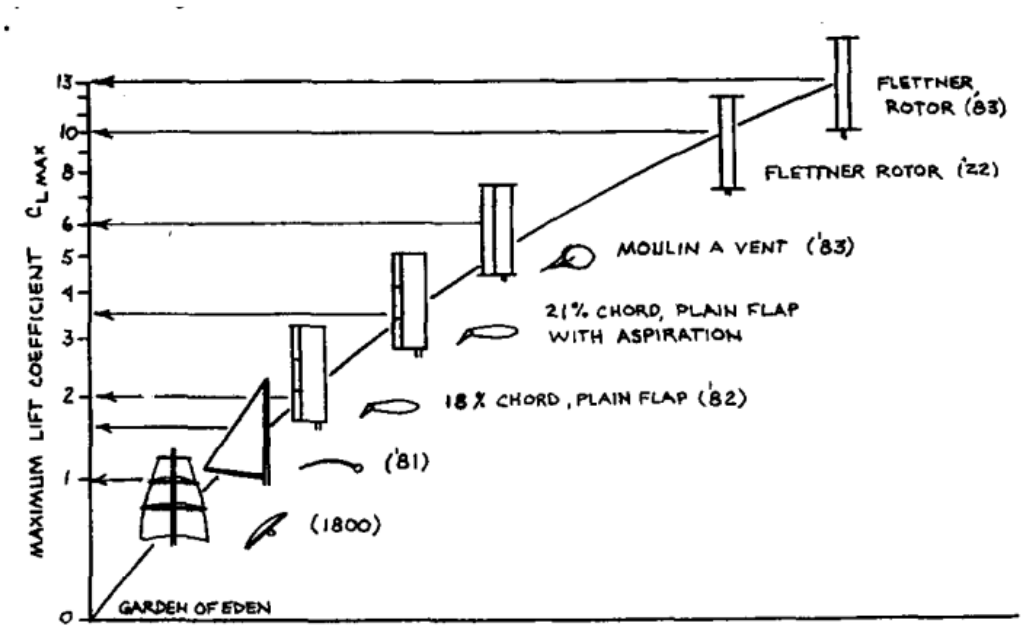

figure 2.5: Maximum Lift Coefficients for Different WASPs (Bergeson)

2.4.1 Criteria Points

The Criteria points as seen in the Score-matrix, are not all suitable for the 'Calculation' method. Because both the Flettner rotor and the Turbosail are made of similar material, have about the same size and volume, can be located at a similar position of the ship and there matureness is almost equal, the criteria points for the objective study can be summarized as: Cost, Performance, Wind load and Impact on Stability.

2.4.1.a *Cost*

The best WASP within the concept will be chosen based on the best *Return On Investment*, hereafter referred to as ROI. The main thesis can be answered by comparing the ROI of the concept with that of a conventional ship. The cost analysis of the concept has been done by taking into account the Initial investment of the design in terms of *construction and labour costs*, hereafter referred to as CONX. Than the *operation costs*, hereafter referred to as OPAX, will be taken as the cost of fuel necessary for the trip duration. As opposed to both the CONX and the OPAX the profit has been estimated by looking at the cargo value.

2.4.1.b *Performance*

The second criteria is 'Performance' which is divided into a maximum lift coefficient and a lift-to-drag ratio. Although the calculations as seen in *paragraph 2.1.1. Lift*, can be used to obtain the *Lift force* (F_L), the calculation would be far too complex. In practise the lift force will often be obtained by using wind tunnel models, and a set of expansive equipment to obtain the dimensionless coefficients, the *lift coefficient* (C_L) and the *drag coefficient* (C_D). *Equations 2.7 and 2.8* show how these coefficients can be multiplied with q and the *reference area* (S) to lead to the appropriate forces.

$$F_L = C_L \cdot q_a \cdot S \tag{2.7}$$

$$F_D = C_D \cdot q_a \cdot S \tag{2.8}$$

Figure 2.6 shows the directions of the *Drag force* (F_D), *Lift force* (F_L) and the resulting force (F) is always in a cross-direction with the gas flow direction.

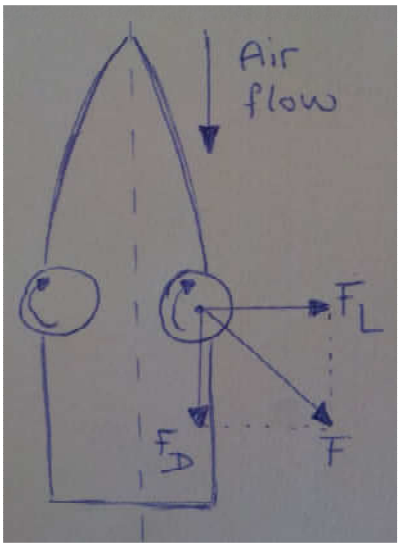

Figure 2.6: Forces as the result from the Air flow (Own Interpretation)

The use of wind tunnel tests often show that the C_L and C_D depend on the flow state of the surrounding gas. This is often expressed in a Reynolds number (Re). As seen in *equation 2.9* the Re depends on the *reference length* (L) and the *kinematic viscosity* (ν in m^2/s). With these parameters the performance can be expressed as the C_L and C_D of the WASP, which must be taken at the appropriate Re.

$$Re = \frac{U \times L}{\nu} \tag{2.9}$$

2.4.1.c *Wind Load*

The performance of the WASP highly depends on the interaction between the WASP and the wind. Because L becomes the result of the gas flow around the body the wind must have a positive *flow velocity* (V_f in m/s) of the gas to get an actual F_L and the *drag force* (F_D in kN).

There is however a difference between the *true wind velocity* (W in m/s) and the *apparent wind velocity* (U in m/s), caused by the ship velocity (V in m/s). This also leads to the difference between the *true wind angle* (ψ_t in degrees) and the *apparent wind angle* (ψ_a in degrees). The geometric relationships between W, U, and V, as seen in *figure 2.8*, can be derived using the Law of Cosines. U and ψ_a can be obtained by using *equations 2.10* and *2.11*, with $U \neq 0$ and $0 \leq \psi_t \leq 180$.

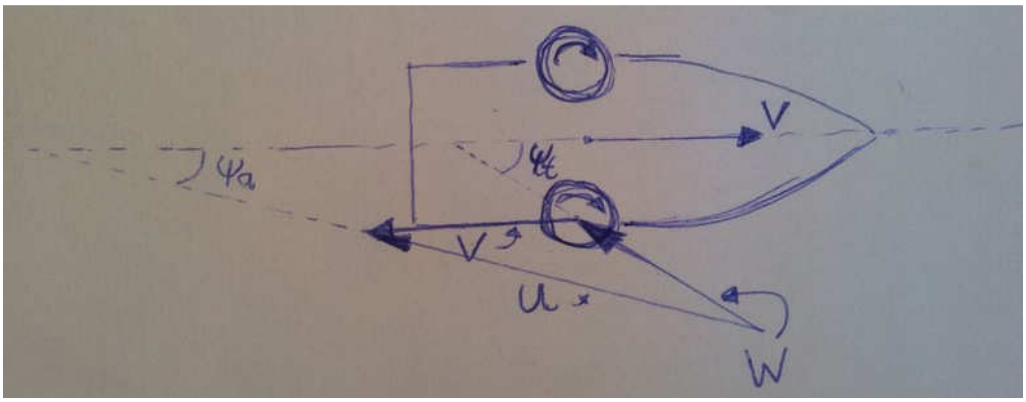

Figure 2.8: True and Apparent Wind Speed and Direction (Own Interpretation)

$$U = \sqrt{W^2 + V^2 + 2WV\ \cos(\psi_t)} \tag{2.10}$$

$$\psi_a = \cos^{-1}\left(\frac{U^2 + V^2 - W^2}{2UV}\right) \tag{2.11}$$

The wind speed[I] in this study has often been given in *Beaufort numbers* (B_n). The relation between W and B_n can be seen in *equation 2.12* [II]

$$W = 0{,}836{B_n}^{1{,}5} \tag{2.12}$$

2.4.1.d *Impact on Stability*

'Impact on stability' represents the amount of heeling moment that the WASP at a specific wind load will cause. The combination of lift and drag forces together forms the *resulting force* (F in kN) of the WASP. The *resulting force coefficient* (C_F) as seen in *figure 2.10* can be obtained by using Pythagoras' theorem, as seen in *equation 2.13.*

[I] Regarding this and the following cf. Kimball (2010)
[II] Which is a simplified version of the formula provided by Kimball (2010), pp. 12f

$$W = 0{,}836B_n\sqrt{B_n}$$

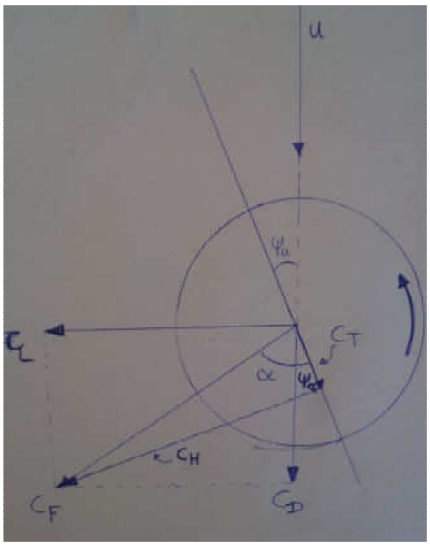

Figure 2.10: Heel, thrust, lift and drag vectors as the result from the wind direction and the heading of the ship (Own Interpretation)

$$C_F = \sqrt{{C_L}^2 + {C_D}^2} \tag{2.13}$$

Figure 2.10 also shows the *heel coefficient* (C_H) and the *thrust coefficient* (C_T). These vectors depend on the angle of attack and the ships heading and can be obtained by using *equations 2.14 and 2.15*, where they depend on the *tangential angle between C_L and C_D* (α in °), which can be obtained by using *equation 2.16.*

$$C_T = -\cos(\alpha + \psi_a) \times C_F \tag{2.14}$$

$$C_H = \sin(\alpha + \psi_a) \times C_F \tag{2.15}$$

$$\alpha = \tan^{-1}\left(\frac{C_L}{C_D}\right) \tag{2.16}$$

The heel force will cause the ship to heel due to the *heel moment* (M_H in kNm) which can be calculated using *equation 2.17.* The *arm* of this *moment* (r_h) can be calculated using *equation 2.18* and is the distance between the *centre of mass of the WASP above the keel* (KG_{wasp}) and the position at half T in m.

$$M_H = F_H \cdot r_h \tag{2.17}$$

$$r_h = KG_{wasp} - 0{,}5 \cdot T \tag{2.18}$$

3 Design Initiation

The new set of design parameters requires an analysis of a reasonable amount of HFSSs. But such designs and parameters have not been available at the duration of this thesis.

However, because the specific HFSS with a WASP is at its core a combination of a sail ship and a *Conventional Freight Sailing Ship*, hereafter referred to as CFSS the hull form must be a combination of the two.

Like a sail ship, the concept should have reliable seakeeping capabilities even under constant heel. This often requires a keel for ballast, or a wider beam on the waterline to increase the position of the *transverse metacentric height* (GM_t).

Sail ships show better streamline than a cargo ship. Sail ships often give up comfort (space) for better sail performance while a cargo ship is mostly defined by the needed cargo space. A cargo ship designer must always add a maximized cargo space for transportation of as much cargo as possible in a ship that is as small as possible. This is an everlasting struggle between the investment costs plus the operational costs and the desired ROI. The desired break-even point depends on multiple design boundaries which have been obtained by determining equal parameters for a comparison between the HFSS and a CFSS plus the boundaries for the WASP criteria points. Although the sub question:

How will the hull from the HFSS differ from that of the CFSS to compensate for the additional aerodynamic forces on the ship?

Will be answered in *chapter 4*, some questions must be answered before the hull form can be obtained. These questions will be answered in this chapter.

- ***What does the operational profile of the Concept look like?***
- ***What freight ship or basic hull will be used for the Concept?***
- ***What will the concept include?***

3.1 Conventional Comparison Ship

The operational profile of the concept has been obtained by determining the operational profile of the comparison CFSS. The operational profile has been expressed as a description of the ship type, cargo and region of operation as well as the service speed.

In this study the CFSS the AMELAND has been used for that purpose . This general cargo ship, as seen in *figure 3.1* has the main particulars as given in *table 3.1*. The ship itself is a coaster, mainly sailing at the North Sea. The specified type of cargo varies from containers to pipes to bulk cargo. The AMELAND can use a tween deck to fit those pipes. These different types of loading cases can be seen in *figure 3.2*. The AMELAND has the possibility to sail at eco-speed, which is 13 kts. This velocity will be maintained within the project for the concept.

Figure 3.1`: The General Cargo Ship 'AMELAND'
(http://imageshack.us/a/img19/4326/amelandnok8513cr2.jpg)

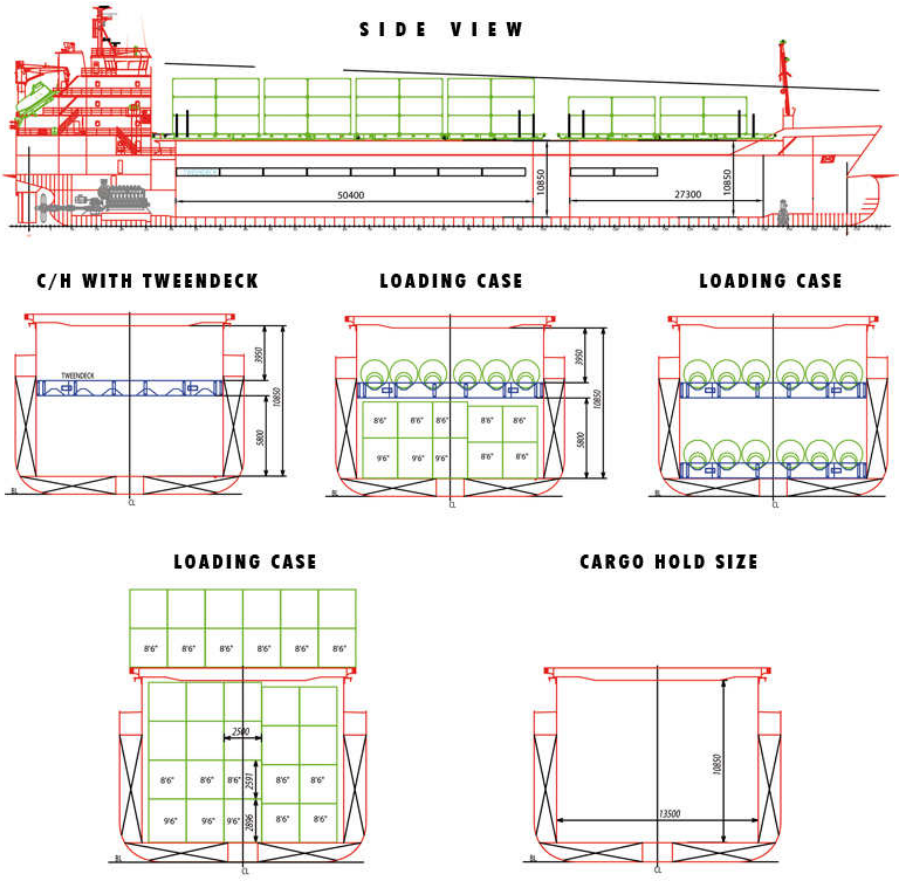

Figure 3.2: Load cases of the AMELAND (http://www.amelandshipping.nl/?page_id=17)

Particulars	Values	Unit
L_{oa}	122,1	[m]
L_{pp}	115,4	[m]
B	16,6	[m]
T	7,2	[m]
D	10,01	[m]
DWT	7610	[t]
P_{MCR}	4000	[kW]

Table 3.1: Particulars of the AMELAND (Own Interpretation)

Unfortunately the data of the AMELAND available for this study does not provide a value of *displacement* (Δ in tons). This is a necessary parameter within the resistance calculation of the ship. Therefore a list of comparison ships with a given displacement have been used to tweak the ICALC. More details about the comparison ships, that have been used to assess the ICALC, can be seen in *Appendix C*, while the verification method of the given particulars of the list of comparison ships can be found in *Appendix D.*

The ICALC has been the result of the outcome of the comparison ships. The hull parameters of the comparison ships have been calculated as described in *Appendix F1*. *Appendix F2 to F8* present the calculation method and results of the resistance calculation for the comparison ships. The calculation method and results for the comparison ships of the weight calculation can be found in *Appendix G1 and G2* with the calculations of respectively the *Light Ship Weight*, hereafter referred to as LSW and the *Deadweight*, hereafter referred to as DWT. The stability calculation method and results of the comparison ships can be seen in *Appendix H.* The results from these calculations have been used to adjust the ICALC method, as can be seen in *Appendix I.* As the result from this calculation, the AMELAND should have the hull and weight particulars as presented in *table 3.2.*

Particulars	Values	Unit
C_B	0,827	[-]
C_M	0,988	[-]
C_P	0,837	[-]
C_{WL}	0,888	[-]
S_W	3167	[m^2]
LSW	4321	[t]
Δ	11931	[t]

Table 3.2: Hull and Weight Particulars of the AMELAND as the Result from the 'Calculation' Method

3.2 Basic Hull Form

Although the AMELAND will be used as the comparison CFSS, her hull form will not be used as the basic hull form for the hybrid concept. A better hull form would be that of the Ecoliner concept, currently at the drawing boards of Dykstra Naval Architects, as seen in *figure 3.3* This HFSS uses a Dyna-rig system as an additional propellant. The Econliner shows an unusual freight ship hull form.

The height of the forecastle deck has been maximized which gives the idea of a low deckhouse. The stern has a round shape, which reminds of traditional sail yacht stern shapes. As this ship is in a further design stadium the hull form has been taken as well optimized. Unfortunately the specific hull coefficients have not been available during the course of this project. Therefore the rough outline of the Ecoliner will be used to tweak the ICALC method even further, which has resulted in a hull form description at the end of this thesis. A remark about the Ecoliner is the absence of any bilge keel. Because a deep analysis of ship motion for the HFSS falls outside the demarcation it has been uncertain whether this should be fitted.

Figure 3.3: Ecoliner Concept, Designed at the Office of Dykstra Naval Architects (http://www.ontdekdenhelder.com/2012/11/06/ecoliner-het-schip-van-de-toekomst/)

3.3 Concept Description

The design should direct toward a concept that fits the needs of the ship type. Because the use of a WASP on the deck limits the amount of cargo that the ship can hold, the general cargo ship type has been chosen. This makes it easy to transport other, more fitting cargo. However, this study will be using containers as the cargo type to calculate the stability and weight, in case a limited amount of containers will be fitted on the main deck of the ship.

The *General Arrangement*, hereafter referred to as GA shows that the design has been depicted with the container-layout.

Because the *height of the WASP* (H_m [m]) limits the visibility in a deckhouse situated aft of the WASP, the deckhouse has been placed in front of the WASP. But the height of the deckhouse will be blocking most of the wind while attributes on top of the deckhouse will most likely cause the wind to be turbulent. Therefore enough space between the deckhouse and the WASPs has been obtained by placing the WASPs on the poop deck. As the result of this design choice the number of container rows on the main deck has to be limited so as not to block the wind for the WASPs. For this study the number of containers rows has been limited to 2.

Because the design of the HFSS tends to be ‘green’, the upcoming changes in rules regarding emissions has lead to the use of the clean fuel type, LNG as the fuel type for the main engine. Like the conventional ship, the HFSS will be using one main engine. The LNG has been stored in standard cryogenic storage units available at Wärtsila. The cryo tanks have been fitted above the main deck on the aft part of the ship because this maximizes the volume of the cargo hold.

Each separate mast will be using a generator for separate power demand, which will run on *Marine Diesel Oil*, hereafter referred to as MDO.

The Ecoliner as seen in *figure 3.3* shows a maximized L_{wl}. This has been done for the concept as well because this would result in a sharper i_E and a lower *Froude number* (F_n) and lowers the wave-making resistance. Lowering the resistance will result in less fuel because of less consumption of the *Main Engine*, hereafter referred to as ME. This will also result in a more environment-friendly design than the CFSS. A third reason is that the maximum L_{wl} will help course keeping because its higher inertia in comparison to a shorter L_{wl} design will minimize the amount of yaw. Another feature to the ship, to minimize the yaw is the adaptation of a skeg. This will protect the propeller and rudder when the ship trims in shallow waters.

A sketch of the concept, depicted with the Flettner rotor, can be seen in *figure 3.4.* This has been the GA goal within the project.

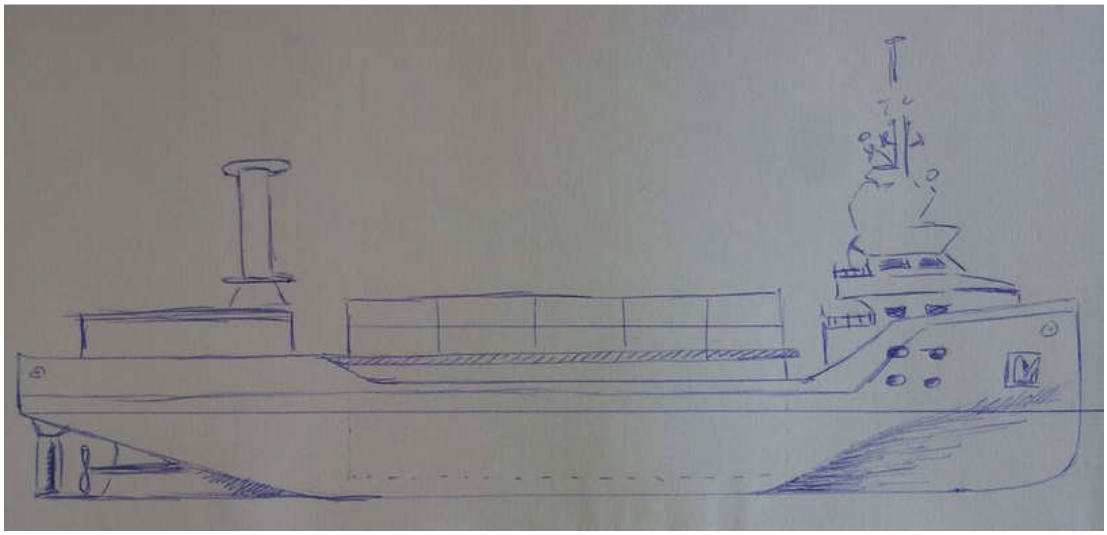

Figure 3.4: Hand Drawing of the General Arrangement (Own Interpretation)

4 Concept Calculation

The design spiral, as seen in *figure 4.1*, represents all the different phases during the basic and concept design of any ship. The continuous loop of calculations or phases leads to the correlation of all the phases and provides the final design parameters as their correlation outcome. Although the ICALC does not include the structure and damage stability phases, the ICALC can be seen as a continuous loop of the spiral. This happens when the outcome of a calculation has been implemented into an earlier calculation step. By using excel for this calculation, the iteration mode could be used to feed the data back to previous calculations.

As described in *paragraph 3.2 Basic Hull Form*, the absence of a decent hull form results in the need to calculate the most effective hull form within the ICALC. *Figure 4.1* shows that the hull form is one of the first phases in the design spiral. Although there have not been sufficient comparison ships to estimate the hull form of the HFSS, the ICALC has been based upon comparison ships. Normally specific ratio's from the comparison ships can be used to estimate how the hull form of the new design will look. Within this project the comparison ships have been used to assess the ICALC method, as described in *Appendices C, D, F, G, H and I*. This verification of accuracy was needed so that the outcome for the HFSS calculation can be trusted as well.

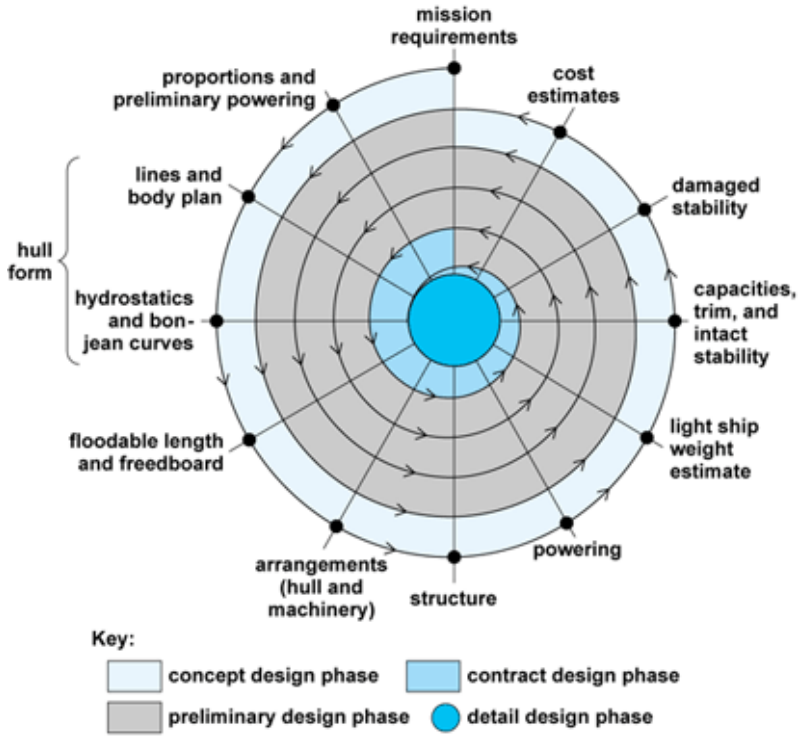

Figure 4.1: Design Spiral (http://pkboatplans.blogspot.nl/2011/11/design-spiral.html)

The outcome of the ICALC as presented in this chapter, have been the result of comparing the results of different *waterline lengths* (L_{wl} [m]), *max breadth of the ship* (B [m]) and H_m.

4.1 Performance

Values of the C_L for the comparison of the WASPs have been based upon the performance parameters as described in the work of Charrier et al[I]. This has been done because it is the only reliable source of Turbosail performance data. It also provides a *power insertion coefficient* (C_a) that gives an idea of how much power needs to be inserted into the WASP to obtain a specific C_L, as seen in *figure 4.3.*

Figure 4.3 suggests that the Turbosail is more efficient in its use of C_a. Up to approximately 6,5 C_L the Turbosail needs less insertion power. The C_D coefficient that comes at the range as provided in *table 4.1,* has been obtained from the study of multiple experts and can be found in *Appendix E.*

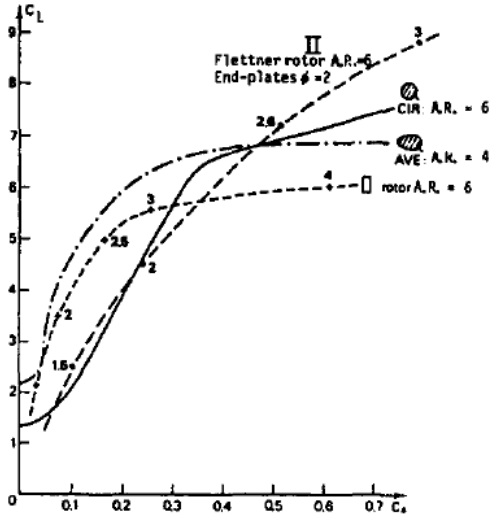

Figure 4.3: Comparison of the power necessary for the working of Flettner rotors and thick aspirated profile wings. (Charrier et al.)

WASP	Flettner rotor		Turbosail	
C_L	C_D	C_p	C_D	C_p
2	0,74	0,08	0,78	0,03
3	0,77	0,13	1,01	0,05
4	0,86	0,2	0,89	0,07
5	0,92	0,29	0,77	0,12
6	1,23	0,38	0,85	0,21

[I] Regarding this and the following cf. Charrier et al. (1985)

7	1,46	0,48	-	-
8	1,23	0,64	-	-

Table 4.1: Usable Lift Coefficient Range for Both WASPs Within the Calculation Method (Own Interpretation)

Because the concept has not been allowed a *heel angle* (ϕ in °) beyond 20°, the WASP will not be able to cause C_{Lmax} all the time. This depends on the wind load in terms of wind force, which is the result of U. Using *equations 2.14* to *2.18* the allowable C_L at a ψ_t of 60° for both WASPs can be seen in *figure 4.4.* This shows that the minimal available C_L can be used at the maximum wind condition of 10 Beaufort.

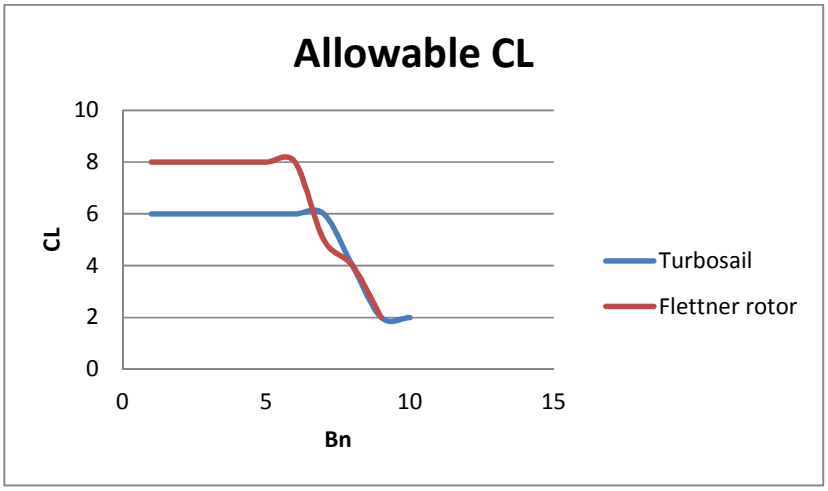

Figure 4.4: Allowable C_L at a wind angle of 60 degrees for both WASPs (Own Interpretation)

The ICALC method provides the design C_L by taking the C_L with the least amount of average resistance. The project has been focussing on adding the best performance available of the WASPs. The design C_L depends on the resistance and thus on the Length-Beam ratio. *Table 4.2* shows the design C_L per length of the ship, at a beam of 20.4 m. The height of the mast for each WASP also affects the amount of design C_L. *Table 4.3* shows the design C_L at various mast heights on a ship with a beam of 20.4 meters and a length of 140 meters. The effect of the numbers of masts on the design C_L for the concept with a length of 140 meters and a beam 0f 20,4 meters can be seen in *table 4.4.*

	L_{wl}			
	134	**137**	**140**	**143**
Flettner rotor	2	8	8	8
Turbosail	6	6	6	6

Table 4.2: Design lift coefficient for the WASPs at Various Length of the Waterline, with a beam of 20,4 meters and two WASPs with a mast height of 18 meters (Own Interpretation)

	H_m			
	16	**18**	**20**	**22**
Flettner rotor	5	2	7	7
Turbosail	2	6	6	6

Table 4.3: Design lift coefficient for the WASPs at Various heights of the mast and with a L_{wl} of 140 meters and a B of 20,4 meters (Own Interpretation)

	n_{WASP}			
	1	**2**	**3**	**4**
Flettner rotor	2	8	7	8
Turbosail	2	6	6	6

Table 4.4: Design lift coefficient for the WASPs at Various number of masts installed and with an L_{wl} of 140 meters and a B of 20,4 meters (Own Interpretation)

4.2 Hull Form

The ICALC method of hull form calculation has been in accordance with the method for the AMELAND with a difference in the method of obtaining C_M. The method can be found in *Appendix J*.

The hull form in terms of dimensions has been tabulated in *table 4.5* for the AMELAND and the concept with the Flettner rotors and the Turbosails. The dimensions have been the result on the cost estimation, where the input of L_{oa}, L_{wl}, and B, and the calculation of the corresponding *draught* (T [m]) to match the appropriate Δ has been used to obtain the most profitable solution.

The beam of the ship has been determined mostly by the stability input. The boundary condition for the dynamic stability has been a max ϕ of 20°. Another choice within the project has been the appliance of the design C_L up to a B_n of 5. Higher wind speeds will demand a lower thrust from the Flettner rotor or the Turbosail to stay within the stability criteria. L_{wl} has been obtained by comparing the financial result from multiple L_{wl} solutions.

Particular	AMELAND	Flettner rotor	Turbosail
L_{wl} [m]	117	140	140
B [m]	16,6	20,7	20,6
T [m]	7,2	7,25	7,2
S_W [m^2]	3167	3295	3302

Table 4.5: Hull Dimension Comparison of the AMELAND and the Concept (Own Interpretation)

The coefficients, as seen in *table 4.6* show that the concept has less length to beam ratio as that of the AMELAND. This is necessary for the stability criteria. The concept has an emphasis on reducing the resistance in comparison to the AMELAND as can be concluded from the lower F_n, C_B, C_P and C_{WL}. These coefficients describe a hull form with less volume at the aft and forward parts of the ship and less waterline area, which results in a slender body under the waterline, in comparison to that of the AMELAND. The difference between the hull form with the Flettner rotor and with the Turbosail is marginal.

Particular	AMELAND	Flettner rotor	Turbosail
L_{wl}-to-B	7,1	6,8	6,8
C_B	0,827	0,563	0,569
C_M	0,988	0,944	0,944
C_P	0,837	0,596	0,603
C_{WL}	0,888	0,744	0,751
F_n	0,197	0,180	0,180

Table 4.6: Coefficient Comparison Between the AMELAND and the Concept (Own Interpretation)

4.3 Weight Calculation

The weight calculation and the hull parameter calculation has been providing input to each other. Therefore both calculations need to be solved iteratively. The Weight calculation has been divided into the estimation of the *Light Ship Weight*, hereafter referred to as LSW, tank capacities and combining this with the desired *deadweight*, hereafter referred to as DWT. The resulting Δ can then be used to re-estimate the C_B in the hull parameters calculation, which will affect the calculation of C_P and the *wetted surface* (S_W in m^2).

4.3.1 Light Ship Weight

The calculation of the LSW of the concept with the WASPs has been done in a similar way as the calculation of the LSW of the comparison ships, as seen in *Appendix G1*. The

differences in the calculation method can be seen in *Appendix K.* The calculation of the HFSS and the CFSS has resulted in the values as seen in *table 4.4.*

Parameters	AMELAND	Flettner rotor	Turbosail	Unit
LSW	4321	4565	4571	[t]

Table 4.7: LSW Results of the Concept and the AMELAND (Own Interpretation)

4.3.2 Deadweight

Due to the higher beam the concept is, as seen in *table 4.8* able to carry more cargo in comparison to the required displacement. This is caused by the difference in volume of the concept in comparison to that of the AMELAND while the LSW is almost the same.

The containers used in the project can be filled up to a maximum weight of approximately 24 tons. Due to stability problems, the containers have been filled as a percentage of that weight, as seen in *Table 4.9.*

Parameters	AMELAND	Flettner rotor	Turbosail	Unit
W_{cargo}	4785	5916	5922	[t]
Δ	11931	12175	12181	[t]
DWT-to-Δ	0,64	0,63	0,63	[-]
W_{cargo}-to-DWT	0,63	0,78	0,78	[-]

Table 4.8: LSW Results of the Concept and the AMELAND (Own Interpretation)

Parameters	AMELAND	Flettner rotor	Turbosail	Unit
Capacity in the cargo hold	240	232	232	[#]
Capacity on the main deck	144	132	132	[#]
Total capacity	384	362	362	[#]
P_{fill} cargo hold	65	70	70	[%]
P_{fill} main deck	5,6	52,1	52,2	[%]

Table 4.9: Cargo weight specifics of the concept design and the AMELAND (Own Interpretation)

4.3.2.a *Fuel*

The HFSS concept will be including an engine that runs on LNG. This makes the design more suitable for coming rules regarding emissions. The savings on emissions of the concept in comparison to the AMELAND have been calculated by using the emissions as specified in *table 4.10.* Using these values on the power results at Beaufort 5, as seen in

*table 4.*11, results in the savings on emissions for the concept in comparison to the AMELAND as seen in *table 4.12.* This is with a trip duration of 984 hours.

Parameters	LNG	HFO	MDO	Unit
NOx	1,4	14	13,2	[g/kWh]
SOx	0	11,5	4,1	[g/kWh]
CO_2	469	677	645	[g/kWh]
HC	0	0,5	0,5	[g/kWh]

Table 4.10: Emissions in grams per kilowatt hour of the different Fuel Types (Own Interpretation)

Parameters	AMELAND	Flettner rotor	Turbosail	Unit
ME	3112	1538,0	1580,5	[kW]
WASP	-	33,9	26,1	[kW]

Table 4.11: Main Engine Power Demand In Upright Condition Without a Wind Load (Own Interpretation)

Parameters	Flettner rotor	Turbosail	Unit
NOx	50,4	52,7	[%]
SOx	49,8	52,2	[%]
CO_2	50,5	52,7	[%]
HC	50,5	52,8	[%]

Table 4.12: Savings on Emissions of the Concept in Comparison to the AMELAND (Own Interpretation)

The LNG will be stored in cryogenic tanks that will be placed above the engine room under the poop deck. A lower position of the tanks could only be obtained by placing the tanks on the tank top in which case it would reduce the cargo hold volume. *Table 4.13* shows the LNG tank specifics for the concept necessary to store the amount of fuel for the 140 meter configuration as seen in *table 4.14.*

LNG Tank	Flettner rotor	Turbosail	Unit
Length	19	19	[m]
Diameter	3,6	3,6	[m]
quantity	3	3	[#]
Weight/unit	53	53	[t]

Table 4.13: LNG Tank Specifics in Accordance with the ICALC outcome (Own Interpretation)

	Fuel Type	L_{wl}			
		134	137	140	143
Flettner rotor	LNG	255	245	245	244
	MDO	3,1	17,6	18,3	17
Turbosail	LNG	249	246	244	241
	MDO	8,9	8,6	8,5	8,5

Table 4.14: Fuel Demand from Multiple L_{wl} Solutions with a B of 20,4 Meters (Own Interpretation)

The resulting power of the *Main Engine* hereafter referred to as *ME*, has been equal for the concept with the Flettner rotor and the Turbosail at a value of 3000 [kW]. That 3000 [kW] engine is a Wartsilä type 34DF with a weight of 23 [t]. The DF stands for Dual-Fuel. This means that a mixture of MDO and LNG must be used to let this engine run. However, this study uses this engine as if it was consuming LNG only. This has been done because the concept is a design for the future, where clean ships will probably be using LNG only.

Because the AMELAND uses MGO as fuel for its generators, the concept will be using MGO for the generators that power the electricity on board. This makes the comparison of the concept with the AMELAND equal. The MGO and HFO specifics of the AMELAND and the concepts can be seen in *tale 4.15.*

Parameters	AMELAND	Flettner rotor	Turbosail	Unit
HFO	500	-	-	[t]
MGO	82,5	82,5	82,5	[t]

Table 4.15: Fuel Capacity Summary of the Concept and the AMELAND (Own Interpretation)

4.3.2.b *Cargo*

The new design will be having an equal DWT to the AMELAND. This means that the total DWT will be approximating 7610 [t]. From the ICALC method follows that the concept can have the cargo hold dimensions as seen in *table 4.16.*

The cargo hold of the AMELAND has been divided by a void, this is most likely the result of the *Heavy Fuel Oil*, hereafter referred to as HFO, that is likely stored in that section. Because the concept does not have to store HFO, the bulkheads have been removed. A calculation of longitudinal stiffening might show that the ship does need a cargo separation, but this has not been determined within the time frame of the study.

Appendix M provides the calculation method behind the cargo hold estimation. The ICALC container capacity at multiple L_{wl} solutions, at a beam of 20,4 meters, can be seen in *table 4.17.* Further details about the obtainment of the cargo hold dimensions and cargo capacity can be seen in *Appendix L*.

Ship	Length [m]	Breadth [m]	Height [m]
Concept	67,80	15,70	11,10
AMELAND	77,70	13,50	11

Table 4.16: Cargo Hold Dimensions of the Concept Design and the AMELAND (Own Interpretation)

	Weight	L_{wl}				Units
		134	137	140	143	
Flettner rotor	Total TEU	336	330	336	324	[#]
	% max load in hold	70	70	70	70	[%]
	% max load on deck	52,3	57	52,5	60,8	[%]
Turbosail	Total TEU	351	345	342	342	[#]
	% max load in hold	70	70	70	70	[%]
	% max load on deck	43	47	49	49	[%]

Table 4.17: Container Specifics for the Concept at Various L_{wl} Solutions (Own Interpretation)

4.4 Stability

As seen in *table 4.5*, the beam of the concept with the Flettner rotor is 20,6 [m] and the beam with the Turbosail is 20,4 [m]. This comes from the stability criteria that ϕ_{max} will not exceed 20°.

Because the ship's loading condition will not be a constant, multiple *loading conditions*, hereafter referred to as LC, have been taken into account. The first LC describes the situation where the containers have been loaded and the tanks are full. The second LC describes the arrival situation with loaded containers, but with almost empty tanks. LC three represents the return of the ship with loaded tanks but with empty containers while LC four is the ship with empty containers and almost empty tanks. *Table 4.18* shows the ICALC GM_t values.

Load cases	Flettner rotor	Turbosail	Unit
LC1	1,27	1,36	[m]
LC2	1,64	1,76	[m]
LC3	2,94	3,00	[m]
LC4	2,01	2,10	[m]

Table 4.18: GMt Values per Load Case for Each WASP Design (Own Interpretation)

4.5 Resistance

The resistance calculation has been based upon the average resistance for a trip duration of 984 hours.

4.5.1.a *Initial Resistance*

The initial resistance situation of the concept can be defined as the upright condition where no force pushes the ship sideways. In that situation the *total resistance* (R_T [kN]) in calm water consists out of *air resistance* (R_{air} [kN]) and *water resistance* (R_{water} [kN]). Of these groups, the R_{water} is the most complex. This group holds, as seen in *figure 4.5* the *frictional resistance* (R_F [kN]), and the *residuary resistance* (R_R [kN]) that consists out of the *pressure resistance* (R_p [kN]) and the *wave making resistance* (R_W [kN]).

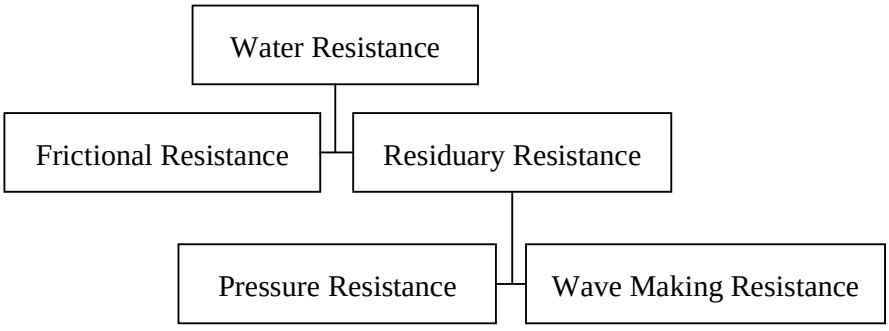

Figure 4.5: Resistance Break-Down Structure (Van Rietbergen)

The R_{water} of the design has been done by using the method of Holtrop (1982), which has been a revised version of his work with Mennen in 1982. The method can be seen in *Appendix F2 to F8*, where the calculation has been done for the comparison ships.
The R_{air} in the upright condition would be measured by taking the *dynamic pressure of the* air (q_{air} [kN/m^2]) as the pressure on the frontal wind area of the ship. However, the inclusion of the WASP into the concept will be requiring the use of the pressure on the side of the ship. *Table 4.19* shows the resistance components as calculated in the ICALC.

Parameters	AMELAND	Flettner rotor	Turbosail	Unit
R_{water}	343	191	193	[kN]
R_{air} (at 5 B_n)	15	18	20	[kN]
R_T (at 5 B_n)	358	209	213	[kN]

Table 4.19: Resistance calculation of the AMELAND and the Concept at 13 kts (Own Interpretation)

4.5.1.b *Resistance due to heel*

The WASP will add a heeling arm to the ship. The R_{water} will be effected because the wetted surface of the hull will be different under heel, as seen in *figure 4.6*. This can either have a positive or negative effect to the overall resistance, but even if the wetted surface would decrease under heel, the manoeuvrability of the ship could be affected negatively due to the position of the rudder. The amount of heel also affects the comfort on board for the crew.

Because no study exists that compares the heel effect of cargo ships with different hull types, a calculation method for estimating the change in wetted surface has been absent. However, this effect has been studied in the sail pleasure industry and the results from those studies have been used to obtain the formulae to estimate the resistance groups due to the WASP for the concept.

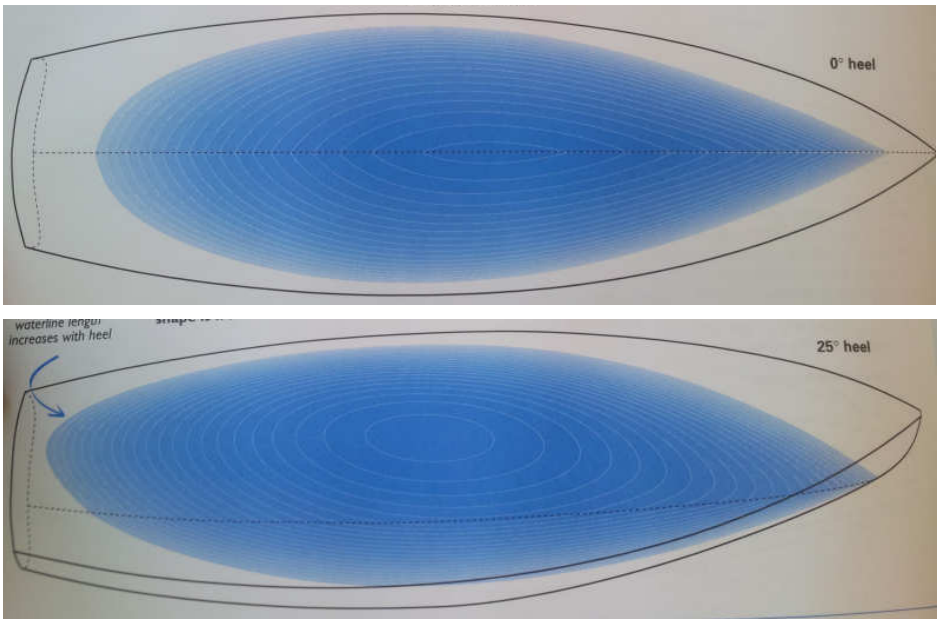

Figure 4.6: Change of the Waterlines due to Heel of a Sailing Yacht (Killing, 1998)

As the result of F_H of the WASP, the ship will heel. This will add resistance that will be summarized as *heel resistance* (R_H). R_H consists out of a change in *hull friction resistance* (R_F) and *additional resistance* (R_a). Under heel, the amount of wetted surface will change and thus will R_F change.

Larsson and Eliasson provide a formulae to obtain the wetted surface at a specific heel angle, by using *equation 3.14* where the s factors in the equation have been obtained by hull model tests of sail yachts. Because the WASP will be installed on a cargo ship, the s factors will be different.

The estimated values have been obtained by analysing the results of an early stage 3D-model of the new design, by giving it various heel angles in the software package Maxsurf. *Appendix N* provides details about the calculation method. The total resistance under heel at various wind angles at Beaufort 5, have been tabulated in *table 4.18.*

Further details about the Resistance calculation can be seen in *Appendix M.*

$$S_{WC\varphi} = S_{WC} \cdot \left[1 + 0{,}01 \cdot \left(s0 + s1 \cdot \left(\frac{B_{WL}}{T}\right) + s2 \cdot \left(\frac{B_{WL}}{T}\right)^2 + s3 \cdot C_{MC}\right)\right] \qquad (3.14)$$

Ψ_t	Flettner rotor	Turbosail	Units
60	217,2	219,9	[kN]
90	217,2	220,1	[kN]
120	217,2	220,2	[kN]
150	210,8	220,2	[kN]

Table 4.18: Resistance Under Heel for the Concept at B_n is 5 (Own Interpretation)

4.5.2 Range

The concept has been designed using a trip duration of 984 hours. This demands an average wind load on the ship for that period of time. The range of the ship in case of no wind has been calculated by using the main engine power demand from the upright resistance calculation in the ICALC and adding 50% additional resistance for waves to the calculation. The results can be seen in *table 4.19.* This shows that there is enough fuel on board to maintain the range. This is because the concept is designed for higher wind loads and thus higher resistance values. Because the concept has been designed to minimize the resistance, she thus has no problem with this 'no windage condition'.

Parameters	Flettner rotor	Turbosail	Unit
ME	2489	2514	[kW]
Consumption	0,0001705	0,0001705	[t/kWh]
Available Fuel	476,7	494,3	[t]
Range	1123,3	1153	[h]
Range loss	None	None	[%]

Table 4.19: Range Calculation in No Windage Condition For the Concept Versions (Own Interpretation)

4.6 3D-Model

Before the cost estimation, a 3D-model has been designed in the MAXsurf model to provide insight into the accuracy of the ICALC method. There is a difference in the outcome of the ICALC and the model, as seen in *table 4.20.* This is mostly due to the change in displacement that has been increased so as to comply with the stability criteria. The required displacement has been obtained by adding an amount of water ballast in the sides of the ships between the hull and the cargo hold. The tank arrangement can be seen in the *Tank Arrangement* drawing.

The model will also be having an additional amount of fuel for the estimation of resistance in rough sea. Because no specific route has been determined the fuel will be doubled. This is possible because of the needed water ballast weight.

The GZ-curves per LC can be seen in *figure 4.7.* In terms of hull coefficients the difference between the numerical calculation and the 3D-model can be seen in *table 4.21.*

After the hull form creation, a simple GA has been set up. This has helped to assess whether the amount of containers can be fitted into the cargo hold.

Particular	Numerical	3D-Model	Units
L_{wl}	140	140	[m]
B	20,7	20,7	[m]
T	7,25	7,03	[m]
S_W	3295	3323	[m^2]
Δ	12175	12382	[t]

Table 4.20: Hull Dimensions of the Concept Maxsurf Model (Own Interpretation)

Particular	Flettner rotor	3D-Model
L_{wl}-to-B	6,8	6,8
C_B	0,563	0,595
C_M	0,944	0,945
C_P	0,596	0,637
C_{WL}	0,744	0,777

Table 4.21: Coefficient Comparison Between the AMELAND and the Concept (Own Interpretation)

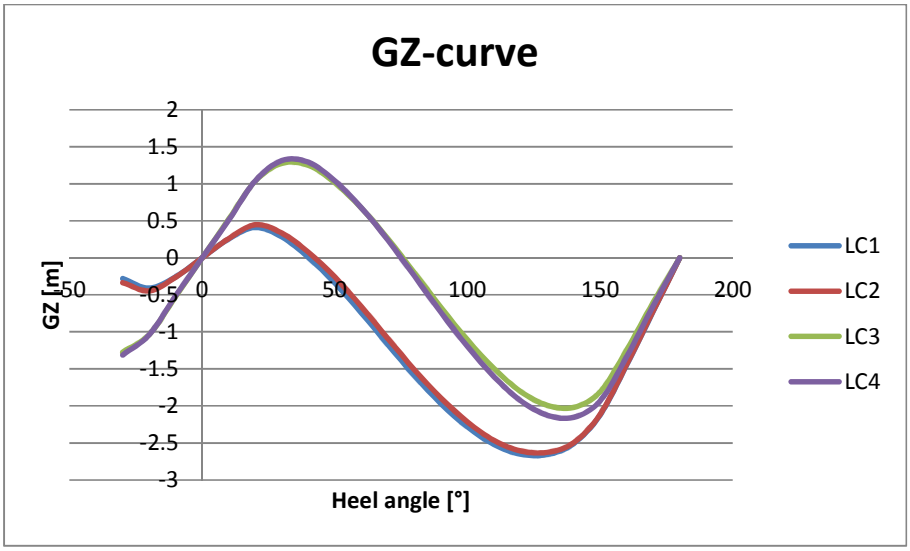

Figure 4.7: GZ-curves of the Concept hull form (Own Interpretation)

The 3D-model has been used to plot the resistance calculation in no-wind condition. This has been compared with the numerical calculation. The curve of the resistance in relation to the ship velocity can be seen in *figure 4.8.*

The ICALC only calculates the resistance at 13 kts. The ICALC provides that the concept version with the Flettner rotor has a resistance at 13 kts of 189 kN. This is exactly what the 3D-model shows. Because the route has not been specified, the required information for a detailed propeller calculation has not been possible. Only the diameter has been estimated by using 0.65 T. This results in a propeller of approximately 4,65 [m].

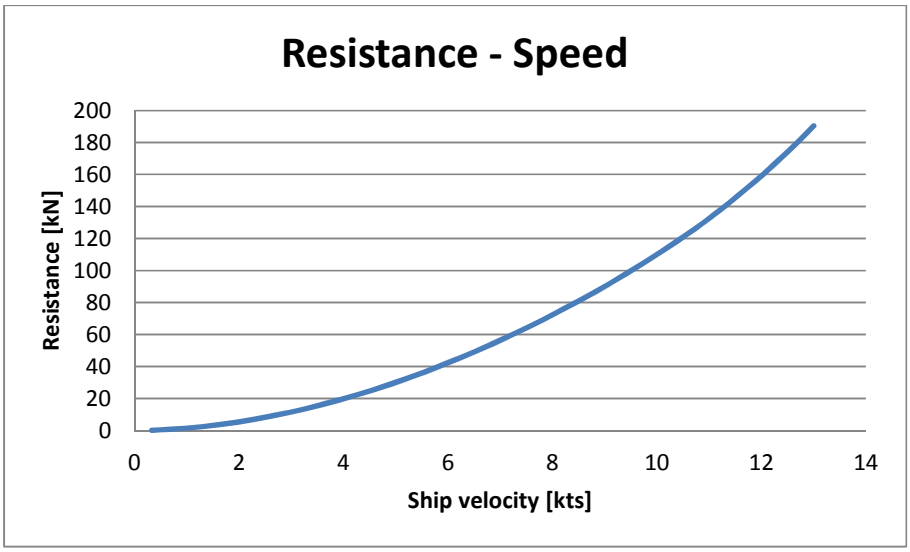

Figure 4.8: Resistance curve from the Maxsurf Model (Own Interpretation)

4.7 Cost

The costs of both WASPs have been compared in a concept version with the dimensions as specified in *table 4.19.* The comparison can be seen in *table 4.22.*

	AMELAND	Flettner rotor	Turbosail	Units
CONX	14.121.056,-	18.115.553,-	16.142.330,-	[$]
OPAX	367.573,-	352.987,-	332.499,-	[$]
Cargo Profit	1.416.000,-	1.418.000,-	1.418.000,-	[$]
ROI	5	7	6	[y]

Figure 4.22: Cost Comparison of the Concept Versions and the AMELAND (Own Interpretation)

4.7.1 Initial Costs

The CONX have been calculated by using the cost of steel per ton and the total steel weight. The costs have been estimated to be 500 USD per ton steel. The costs have been calculated for the concept with a length of 140 meters and a beam of 20,7 meters. The results can be seen in *table 4.23.*

	AMELAND	Flettner rotor	Turbosail	Units
Steel	2841	2786	2837	[t]
Steel cost	1.420.500,-	1.392.784,-	1.418.572,-	[$]

Table 4.23: Steel Cost Estimation (Own Interpretation)

In addition to the steel weight, the ICALC has added the weights as seen in *table 4.24.*

	AMELAND	Flettner rotor	Turbosail	Units
Labor	123.343,-	138.116,-	141.354,-	[$]
Weld	3.167,-	3.549,-	3.638,-	[$]
Paint	21.996,-	26.122,-	26.717,-	[$]
Additional	12.552.050,-	12.552.050,-	12.552.050,-	[$]
WASPs	-	2.000.000,-	2.000.000,-	[$]

Figure 4.24: Additional CONX Costs of the AMELAND and the Concept Versions (Own Interpretation)

4.7.2 Operational costs

The operational costs have been obtained by using the amount of fuel and the costs per tones of fuel. The costs per fuel can be seen in *table 4.25*, while the results of the operational costs can be seen in *table 4.26.* These values have been based upon the amounts of fuel as seen in *table 4.27.*

Fuel		Units
LNG	500	[$/t]
MDO	913	[$/t]
HFO	584,5	[$/t]
MGO	913	[$/t]

Figure 4.25: Fuel cost per Tons (Own Interpretation)

Parameters	AMELAND	Flettner rotor	Turbosail
LNG	-	246.365,-	255.657,-
MDO	-	31.300,-	1.519,-
HFO	292.250,-	-	-
MGO	75.323,-	75.323,-	75.323,-
Total	367.573,-	352.988,-	332.499,-

Table 4.26: OPAX of the AMELAND and the Concept Versions at L_{wl} of 140 meters and B of 20,4 meters (Own Interpretation)

Parameters	AMELAND	Flettner rotor	Turbosail
LNG	-	493	511
MDO	-	34,3	1,7
HFO	500	-	-
MGO	82,5	82,5	82,5

Figure 4.27: Fuel Capacities for the Concept and the AMELAND (Own Interpretation)

5 Results and Recommendations

The main goal of this study has been to answer the question:

Is an application of the Magnus-effect in a hybrid sailing concept invest worthy in comparison with a conventional ship by equal operational profile?

From the costs comparison can be concluded that the Turbosail has a shorter ROI than the Flettner rotor. The interesting outcome from the cost estimation is that the concept has about the same results as that of the AMELAND, as seen in *figure 5.1*. This is however the result with a Turbosail that has a lower design C_L of about 2. The Flettner rotor has a C_L design of 8. Although the thesis does not specify the amount of design C_L, the outcome will be compared on the max available C_L. This means that the Turbosail is not performing at the maximum available performance.

Therefore the Flettner rotor will be chosen as the best suitable WASP for the hybrid concept, if the max available C_L is an additional criteria point.

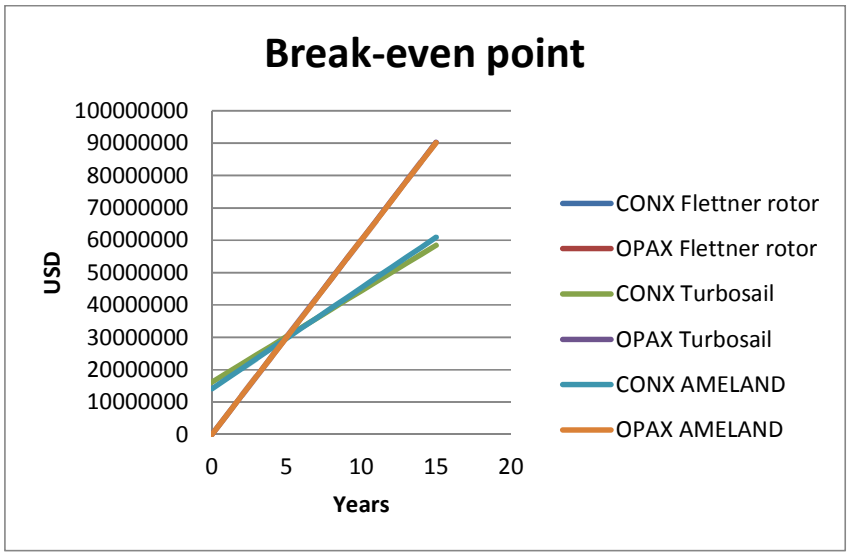

Figure 5.1: CONX and OPAX of the concept and the AMELAND (Own Interpretation)

The invest worthiness depends on whether the concept has enough revenue at the end of her service time to build a new ship. *Table 5.1* shows that the total profit after 15 years of service is enough to build a new ship. Therefore the answer to the Thesis is:

Yes, an application of the Magnus-effect in a hybrid sailing concept is invest worthy in comparison with a conventional ship at a deadweight of 7610 [t].

	AMELAND	Flettner rotor	Units
Profit	29,2 million	25,9 million	[$]

Table 2.1: Profit After 15 Years of Service (Own Interpretation)

There are some notes to the outcome of this study. The performance data as provided by Charrier et al. is the only available source for data of the Turbosail. Because the document is over 30 years old it is likely that today's technology could improve those performance data. Also the source does not provide information about whether the performance data comes from WASPs implemented on a hull form and what hull form this is. It also does not specify the wind angle or the wind condition.

One of the SAIL partners will be performing a CFD study of the WASPs, and this may hold better improvements to the results of the Turbosail in this study.

The MARIN, as a member of SAIL, will be using the 3D-model to assess the relations between fuel, cost, sail time and emissions within the route software Gulliver. This will be a comparison study on itself. Because the MARIN will be using wave data for existing routes, the concept must gain an additional amount of fuel to overcome the additional resistance. Moreover, the ships movement in rough sea conditions, will be requiring a study of rudder and propeller optimization as well as an estimation of induced drag and course keeping. Most of these problems must be solved through the use of towing tank tests, which will not be realized within the SAIL project.

Further study about the effect of the position of the Flettner rotor on the ship, on the ships motions must be done. This will also require a suitable estimation of the centre of lateral resistance for cargo ships.

Although the study has shown that the WASP could be installed successfully on a hull and comply with stability criteria and be profitable, the financial estimation could be improved by monitoring actual shipping revenue, and applying the results onto the WASP.

The specific hull form and the specific revenue has been obtained for a 7610 ton DWT ship. Studies could be done to assess the hull specifics at higher or lower DWT designs.

Doing this well help all Maritime Engineers, for it will provide the design grid of the future, that of the WASP hybrid designs.

6 Bibliography

6.1 Printed Sources

Barrass, C. B. (2004): *Ship Design And Performance For Masters And Mates*. 1st edition. Elsevier Butterworth-Heinemann.

Barrass, C. B. and Derrett, D. R. (2006): *Ship Stability For Masters and Mates*. 6th edition. Elsevier Butterworth-Heinemann.

Bergeson, Lloyd and Greenwald, C. Kent (1985): *Sail Assist Developments 1979-1985*. Journal of Wind Engineering and Industrial Aerodynamics. Elsevier Science Publishers B.V.

Charrier, Bertrand; Constans, Jacques; Cousteau, Jacques-Yves; Abdallah, Daïf; Malavard, Lucien; and Quinio, Jean-Luc. (1985): *Fondation Cousteau and Windship 1980-1985 System Cousteau-Pechiney*. Journal of Wind Engineering and Industrial Aerodynamics, 28, 39-60.

Ferro R. S. T. and Strange E. S. (1986): *The Use of Spinning Rotors to Manoeuvre a Single Boat Pelagic Trawl*. Department of Agriculture and Fisheries for Scotland Marine Laboratory, Working Paper No 5.

Fossati, Fabio (2009): *Aero-Hydrodynamics And The Performing Of Sailing Yachts*. 1st edition. Adlard Coles Nautical.

Gendron, K. and Trouvé, G. (2013): *Wind Propulsion Technologies Review*. Paper.

Gernez, Etienne (2010): *Wind Propulsion For Ships In 2010: Why So Few?* Paper.

Gowree, E. R. and Prince, S. A. (2012): *A Computational Study Of The Aerodynamics Of A Spinning Cylinder In A Crossflow Of High Reynolds number*. Paper. Centre of Aeronautics, City University London.

Holtrop, J. (1984): *A Statistical Re-Analysis Of Resistance And Propulsion Data*. Paper

Holtrop, J. and Mennen, G.G.J. (1982): *An Approximate Power Prediction Method*. Paper.

Johnson, Claes (2011): *The Secret Of Sailing*. Paper.

Killing, Steve and Hunter, Douglas. (1998): *Yacht Design Explained. A sailor's guide to the principles and practice of design.* 1st edition. W. W. Norton & Company, Inc.

Kimball, John (2010): *Physics Of Sailing*. CRC Press.

Larsson, Lars and Eliasson, Rolf E. (2007): *Principles Of Yacht Design*. 3rd edition. Adlard Coles Nautical.

Schneekluth, H. and Bertram, V. (1998): *Ship Design For Efficiency & Economy*. 2nd edition. Butterworth-Heinemann.

Seifert, Jost (2012): *Progress in Aerospace Sciences*. 1st edition. Elsevier Ltd.

Van Rietbergen, E. (2011): *Weerstand en Voortstuwing I.* Paper. NHL Hogeschool.

Watson, David G. M. (1998): *Practical Ship Design*. Elsevier Ocean Engineering Book Series Volume 1. Elsevier Science Ltd.

6.2 Online Sources

Alward, Joseph F. (n.d.): *Aerodynamic Lift Explained*. URL: http://www.aerodynamiclift.com/ (visited on Sept 24, 2013)

Brandon, Patrick (n.d.): *What Is The Magnus Effect And How To Calculate It.* URL: http:ffden.phys.uaf.edu/211_fall2010.web.dir/Patrick_Brandon/what_is_the_magnus_effet.html (visited on Sept. 16, 2013)

Encyclopaedia Britannica (n.d.): *Clipper Ship*. URL: http://www.britannica.com/EBchecked/topic/121871/clipper-ship (visited on Sept. 30, 2013)

Encyclopaedia Britannica (n.d.): *Magnus Effect*. URL: http://www.britannica.com/EBchecked/topic/357684/Magnus-effect (visited on Sept. 17, 2013)

NASA (n.d.): *Dynamic Pressure.* URL: http://www.grc.nasa.gov/WWW/BGH/dynpress.html (visited on Sept 30, 2013)

NASA (n.d.): *Lift Of Rotating Cylinder*. URL: www.grc.nasa.gov/WWW/k-12/airplane/cyl.html (visited on Sept. 16, 2013)

Project SAIL (n.d.): *Sail Into A Sustainable Future.* URL: http://nsrsail.eu/ (visited on Sept. 2, 2013)

Ventura, Manuel (n.d.): *Estimation Methods for Basic Ship Design*. URL: http://www.mar.ist.utl.pt/mventura/Projecto-Navios-I/EN/SD-1.3.1-Estimation%20Methods.pdf (visited on Oct. 14, 2013)

Windsomnia Blog (2010): *How To Calculate Apparent Wind.* URL: http://www.windsomnia.com/2010/03/28/apparentwind/ (visited on Oct. 1, 2013)

Thiiink (n.d.): *History & Validation*. URL: http://www.thiiink.com/history-of-flettner-rotor/ (visited on March 11, 2014)